EARTHQUAKE SPECTRA

The Professional Journal of the Earthquake Engineering Research Institute

PREPRINT

This preprint is a PDF of a manuscript that has been accepted for publication in *Earthquake Spectra*. It is the final version that was uploaded and approved by the author(s). While the paper has been through the usual rigorous peer review process for the Journal, it has not been copyedited, nor have the figures and tables been modified for final publication. Please also note that the paper may refer to online Appendices that are not yet available.

We have posted this preliminary version of the manuscript online in the interest of making the scientific findings available for distribution and citation as quickly as possible following acceptance. However, readers should be aware that the final, published version will look different from this version and may also have some differences in content.

The DOI for this manuscript and the correct format for citing the paper are given at the top of the online (html) abstract.

Once the final, published version of this paper is posted online, it will replace the preliminary version at the specified DOI.

Size Limitations for Piles in Seismic Regions

Raffaele Di Laora,[a)] George Mylonakis,[b),c),d)] M.EERI and Alessandro Mandolini[a)]

A novel theoretical study exploring the importance of pile diameter in resisting seismic actions of both the kinematic and the inertial type is reported. With reference to a pile under a restraining cap, is shown analytically that for any given set of design parameters, a range of admissible pile diameters exists, bounded by a minimum and a maximum value above and below which the pile will yield at the top even with highest material quality and amount of reinforcement. The critical diameters depend mainly on seismicity, soil stiffness and safety factor against gravity loading, and to a lesser extent on structural strength. This scale effect is not present at interfaces separating soil layers of different stiffness, yet it may govern design at the pile head. The work at hand deals with both steel and concrete piles embedded in soils of uniform or increasing stiffness with depth. Closed-form solutions are derived for a number of cases, while others are treated numerically. Application examples and design issues are discussed.

INTRODUCTION

In recent years, a vast amount of research contributions dealing with the seismic performance of piles has become available. The topic started receiving attention when theoretical studies, accompanied by a limited amount of experiments and post-earthquake investigations, revealed the development of large bending moments: (a) at the head of piles restrained against rotation by rigid caps and (b) close to interfaces separating soil layers of sharply differing stiffness, even in the absence of large soil movements such as those induced by slope instability or lateral spreading following liquefaction (Kavvadas and Gazetas 1993, Pender 1993, Gazetas and Mylonakis, 1998, Brandenberg et al. 2005, Varun et al. 2013 among others). Nevertheless, interpretation of the available evidence is not straightforward

[a)]Department of Civil Engineering, Design, Building and Environment (DICDEA), Second University of Napoli, Aversa, Italy
[b)] Department of Civil Engineering, University of Bristol, UK.
[c)]Department of Civil Engineering, University of Patras, Rio, Greece.
[d)]Department of Civil Engineering, University of California at Los Angeles, US.

given: (1) the simplified nature of theoretical studies with reference to geometry, material properties and seismic input; (2) the difficulty in simulating real-life conditions in lab experiments; (3) the uncertainties associated with interpreting data from post-earthquake investigations to allow development of empirical databases; (4) the superposition of simultaneous kinematic and inertial interaction phenomena, whose effects are difficult to separate. It is noted that the former type of interaction leads to development of bending regardless of the presence of a superstructure, and may be significant over the whole pile length, whereas the latter generates moments that are maximum at the pile top and become insignificant below a certain depth (Figure 1).

A simple method for assessing the kinematic component of pile bending was first proposed by Margason (1975) and Margason and Holloway (1977). These articles can be credited as the first to investigate the role of pile diameter (to be denoted in the ensuing by d) and recommend, with some justification, the use of small diameters to "conform to soil movements." While several subsequent studies investigated the problem (e.g., Mineiro 1990, Kavvadas and Gazetas 1993, Kaynia and Mahzooni 1996, Mylonakis et al. 1997, Nikolaou et al. 2001, Castelli and Maugeri 2009, de Sanctis et al. 2010, Dezi et al. 2010, Sica et al. 2011, Di Laora et al. 2012, Anoyatis et al. 2013), only a handful of investigations focused on the effect of pile diameter, mostly for bending in the proximity of interfaces separating soil layers of sharply differing stiffness (Mylonakis 2001, Saitoh 2005).

Recently, Di Laora et al. (2013) explored the role of pile diameter in resisting seismic actions at the pile top in presence of a cap restraining head rotation, with reference to steel piles in homogeneous soil. The work highlighted that kinematic bending moment is proportional to d^4, and moment capacity to d^3. This observation revealed a previously unsuspected scale effect that causes moment demand to increase faster than moment capacity, thus making yielding at the pile head unavoidable beyond a certain "critical" diameter. Note that this behavior is not encountered in the vicinity of deep interfaces—the topic most investigated in the literature (Mylonakis, 2001, Maiorano et al. 2009, Dezi et al. 2010, Sica et al 2011, Di Laora et al 2012), since in those regions capacity and demand were both found to increase in proportion to d^3. Di Laora et al. (2013) and Mylonakis et al. (2014) also showed that combining kinematic and inertial moments at the pile head leads to a limited range of admissible diameters, the upper bound being controlled by kinematic bending and the lower bound by inertial bending.

Proceeding along these lines, the article at hand has the following main objectives: (1) to expand and generalize the aforementioned work for both steel and concrete piles in homogeneous and inhomogeneous soil, that is, in soils having constant stiffness or stiffness increasing with depth (Figure 2); (2) to provide a number of closed-form solutions for the limit diameters; (3) to assess the practical significance of the phenomenon through pertinent parametric studies encompassing a wide range of commonly encountered design parameters; (4) to propose a simplified evaluation scheme that can be utilized in practice.

The study employs the following main assumptions: (a) the pile is designed to remain elastic during ground shaking (i.e., the force modification coefficients are set equal to one); (b) the pile is long and idealized as a flexural Euler-Bernoulli beam; (c) the pile axial bearing capacity results from both shaft and tip resistance; (d) the pile is perfectly fixed at the head and in full contact with the soil; (e) seismic excitation consists exclusively of vertically propagating shear waves; (f) group effects associated with bending at the pile head, pile buckling, negative skin friction, loading due to slope movements and soil liquefaction are ignored; (g) soil in the free field can be treated as an equivalent linear material having stiffness and damping compatible with the level of induced strain; additional nonlinearities due to kinematic and inertial soil-structure interaction have a minor effect on pile bending moments. This assumption is discussed in detail later in this article. In addition, for the sake of simplicity, partial safety factors are not explicitly incorporated in the analysis (although it is straightforward to scale material parameters by any desired safety factor); global safety factors are employed instead. It is worth mentioning that the approach in (a) has been questioned in recent years (see, e.g., Gajan and Kutter 2008, Gazetas et al. 2013, Millen 2016). Under-designing foundations, however, although promising in certain respects, is not an established design approach and will not be further discussed here.

SIZE LIMITATION FOR STEEL PILES IN HOMOGENEOUS SOIL

Recent studies by de Sanctis et al. (2010), Di Laora et al. (2013), and Anoyatis et al. (2013) have demonstrated that a long fixed-head pile in homogeneous soil experiences a curvature at the top, $(1/R)_p$, which is related to soil curvature, $(1/R)_s$, through the simple equation:

$$\left(1/R\right)_p = \Psi \left(1/R\right)_s \tag{1}$$

where Ψ is a dimensionless coefficient accounting for soil-structure interaction, that varies between approximately 0.9 and 1 depending mainly on frequency and pile-soil stiffness contrast.

Recalling that for vertically propagating shear waves, soil curvature in a homogeneous soil layer is given by $(1/R)_s = a_s/V_S^2$, with a_s and V_S being the soil acceleration and soil shear wave propagation velocity at a specific depth and setting $\Psi = 1$, the kinematic moment at the pile head may be readily computed from the familiar strength-of-materials equation:

$$M_{head}^{kin} = E_p I_p \left(1/R\right)_p \approx E_p I_p \left(1/R\right)_s = E_p I_p \frac{a_s}{V_s^2} \tag{2}$$

where E_p and I_p are the Young's modulus and cross-sectional moment of inertia of the pile (for a circular cross section, $I_p = \pi d^4/64$), and a_s is the acceleration at soil surface. As evident from Equation 2, head moment increases with pile bending stiffness and acceleration, and decreases with soil stiffness.

The above equation also highlights that kinematic moment increases in proportion to the fourth power of pile diameter (d^4). As the moment capacity M_u of a circular cross section made of a uniform material is proportional to the third power of pile diameter (d^3), it follows that kinematic action tends to prevail over section capacity with increasing diameter. This suggests the existence of a *maximum diameter* d_{kin} beyond which the pile will not be able to undertake the kinematically imposed bending moment without yielding at the head.

If one assumes, as a first-order approximation, that the load carried by a pile under working conditions, P_p, is controlled by shaft resistance (which is proportional to d), the inertial moment acting upon a long pile (which is proportional to $P_p \times d$) will increase in proportion to d^2 (Di Laora et al. 2013). Therefore, in light of Equation 2, resisting inertial action requires a *minimum diameter*, d_{in}, the opposite to the previous result. The above preliminary investigation leads to two useful conclusions, as depicted in Figure 3:

1. Kinematic moments at the pile head tend to dominate over inertial moments as the pile diameter increases.
2. Only a limited range of diameters allows resisting both kinematic and inertial loading.

These findings are elaborated in the following section.

YIELD MOMENT

Considering a cylindrical steel pile, the cross-sectional moment capacity can be computed from the well-known formula (Popov 1976):

$$M_y = E_p I_p \varepsilon_y \frac{2}{d}\left(1 - \frac{P_p}{f_y A}\right) \tag{3}$$

ε_y and f_y being the uniaxial yield strain and the corresponding yield stress of the steel material. A is the cross-sectional area and P_p the axial load carried by the pile.

Considering the undrained response of a pile embedded in homogeneous fine-grained soil layer, P_p can be expressed in terms of geometry, soil properties and a global safety factor as (e.g., Viggiani et al. 2012)

$$P_p = \frac{1}{FS}\left[\pi \alpha L d + N_c A\right] s_u \tag{4}$$

where s_u is the undrained shear strength of the soil material, α the pile-soil adhesion coefficient (typically ranging from 0.3 to 1 depending on s_u), N_c the tip bearing capacity factor (varying between approximately 8 and 12) and FS a global safety factor against axial bearing capacity failure.

KINEMATIC LOADING

Equating the kinematic demand moment in Equation 2 to the yield moment in Equation 3 and making use of the axial load P_p given by Equation 4, the following dimensionless equation for the limit pile size is obtained:

$$\frac{1}{2\varepsilon_y}\frac{a_s L}{V_s^2}\left(\frac{d}{L}\right)^2 - \left(1 - T_1\right)\left(\frac{d}{L}\right) + \frac{4\alpha}{q_A FS}\frac{s_u}{f_y} = 0 \tag{5a}$$

where

$$T_1 = \frac{N_c s_u}{q_A FS f_y} \tag{5b}$$

is a dimensionless tip bearing capacity coefficient, $q_A = 1 - (1 - 2t/d)^2$ being a dimensionless geometric factor accounting for wall thickness, t, of a hollow pile.

Equation 5 admits the pair of solutions:

$$d_{kin} = 2\varepsilon_y \frac{V_s^2}{a_s}\left(1-T_1\right)\left[\frac{1}{2} \pm \sqrt{\frac{1}{4} - \frac{2\alpha}{\varepsilon_y q_A FS}\left(\frac{V_s^2}{a_s L}\right)^{-1}\left(\frac{s_u}{f_y}\right)\left(1-T_1\right)^{-2}}\right] \tag{6}$$

the largest of which, corresponding to the (+) sign, yields the critical (maximum) pile diameter to withstand kinematic action and it is the one considered in the ensuing.

If tip resistance, expressed by coefficient T_1 in Equation 6, is neglected and the shear wave velocity, V_S, under the square root is expressed in terms of soil Young's modulus, E_s, Poisson's ratio, ν_s, and mass density, ρ_s (i.e., $E_s = 2(1+\nu_s)\rho_s V_S^2 \cong 3\rho_s V_S^2$), the above solution reduces to the special case reported by Di Laora et al. (2013):

$$d_{kin} = 2\varepsilon_y \frac{V_s^2}{a_s}\left[\frac{1}{2} + \sqrt{\frac{1}{4} - \frac{6\,\rho_s\,\alpha\,a_s L}{\varepsilon_y\, q_A\, SF}\left(\frac{E_s}{s_u} f_y\right)^{-1}}\right] \tag{7}$$

which has the advantage that the term in brackets does not depend on absolute soil stiffness and strength, but only on the ratio E_s/s_u, which typically varies between 10^2 and 10^3. Note that for zero axial load, which implies infinite safety against axial bearing capacity failure ($FS \rightarrow \infty$), the term in brackets in Equations 6 and 7 tends to unity and the solution reduces to the simple expression:

$$d_{kin} = 2\varepsilon_y \frac{V_s^2}{a_s} \tag{8}$$

This result can also be obtained directly from Equations 2 and 3 by setting $P_p = 0$.

INERTIAL LOADING

Considering solely inertial action and assuming, for simplicity, that the lateral load imposed at the pile head is proportional to the axial gravitational load P_p carried by the pile, it is straightforward to show from elementary Winkler theory that the maximum moment at the pile head in presence of a rigid cap is:

$$M_{in} = \frac{1}{4}\left(\frac{\pi q_I}{\delta}\right)^{\frac{1}{4}}\left(\frac{a_s}{g}\right)\left(\frac{E_p}{E_s}\right)^{\frac{1}{4}} S_a\, P_p\, d \tag{9}$$

δ being the Winkler stiffness parameter (which is about 1 to 1.5 for inertial loading; see Novak et al. 1978, Roesset 1980, Dobry et al. 1982, Syngros 2004, Anoyatis et al. 2016, Karatzia and Mylonakis 2016), $q_I = 1-(1-2t/d)^4$ a dimensionless geometric factor accounting

for wall thickness, t, of a hollow pile, S_a a dimensionless spectral amplification parameter, g being the acceleration of gravity.

Equating the right sides of Equations 3 and 9 and employing Equation 4, the following explicit solution is obtained:

$$d_{in} = \frac{8\alpha}{FS\left(1-T_2\right)} L \left[\frac{S_a}{\varepsilon_y} \left(\frac{\pi}{\delta} \right)^{\frac{1}{4}} \left(\frac{a_s}{g} \right) \left(q_1 \frac{E_p}{E_s} \right)^{-\frac{3}{4}} \left(\frac{s_u}{E_s} \right) + \frac{1}{2q_A} \left(\frac{s_u}{f_y} \right) \right] \tag{10a}$$

where:

$$T_2 = T_1 \left[1 + 8 \left(\frac{\pi q_1}{\delta} \right)^{\frac{1}{4}} \left(\frac{a_s}{g} \right) \left(\frac{E_p}{E_s} \right)^{\frac{1}{4}} \frac{S_a q_A}{q_1} \right] \tag{10b}$$

is a second dimensionless tip resistance coefficient.

Equation 10 defines a critical (minimum) pile diameter to withstand inertial action in an elastic manner. It is worth noting that neglecting tip action (i.e., setting $T_2 = 0$), the above result reduces to the simpler solution of Di Laora et al. (2013). In absence of ground acceleration ($a_s = 0$), Equation 10 degenerates to:

$$d_{in} = \frac{4\alpha L}{SF\, q_A} \left(\frac{s_u}{f_y} \right) \frac{1}{1-T_1} \tag{11}$$

which defines the minimum diameter needed to resist the gravitational load P_p by combined tip resistance and skin friction. The same result can also be obtained by setting $a_s = 0$ in Equation 5a.

COMBINED KINEMATIC AND INERTIAL LOADING

For the more realistic case of simultaneous kinematic and inertial loading, Equations 2 and 9 can be combined for the overall flexural earthquake demand at the pile head by means of the superposition formula:

$$M_{tot} = e_{kin} M_{kin} + e_{in} M_{in} \tag{12}$$

where subscript *tot* stands for "total" and e_{kin}, e_{in} are dimensionless correlation coefficients ranging from –1 to 1, that account for the non-simultaneous occurrence of maximum kinematic and inertial actions. For simplicity, and as a first approximation this effect is not considered in the following (i.e., $e_{kin} = e_{in} = 1$).

Setting the total earthquake moment equal to the yield moment in Equation 3, one obtains the following second-order dimensionless algebraic equation for the limit pile size:

$$\frac{1}{2}\frac{a_s L}{V_s^2}\left(\frac{d}{L}\right)^2-(1-T_3)\varepsilon_y\left(\frac{d}{L}\right)+\frac{4\alpha}{q_A SF}\left(\frac{s_u}{E_p}\right)\left[1+2\frac{q_A}{q_I}\left(\frac{\pi q_I}{\delta}\right)^{\frac{1}{4}}\left(\frac{a_s}{g}\right)\left(\frac{E_p}{E_s}\right)^{\frac{1}{4}}S_a\right]=0 \tag{13a}$$

where:

$$T_3=\left[\frac{1}{q_A\,SF\,f_y}+\frac{2}{\varepsilon_y}\left(\frac{\pi}{\delta}\right)^{\frac{1}{4}}\left(\frac{q_I E_p}{E_s}\right)^{-\frac{3}{4}}\left(\frac{s_u}{E_s}\right)\right]N_c \tag{13b}$$

is a third dimensionless tip-bearing capacity coefficient.

Equation 13a can be solved for the pair of pile diameters

$$d_{1,2}=\frac{\varepsilon_y V_s^2}{a_s}(1-T_3)\left\{1\mp\sqrt{1-\frac{24\alpha\rho_s a_s L}{(1-T_3)^2 q_A f_y \varepsilon_y SF}\left(\frac{s_u}{E_s}\right)\left[1+2\frac{q_A}{q_I}\left(\frac{\pi q_I}{\delta}\right)^{\frac{1}{4}}\left(\frac{a_s}{g}\right)\left(\frac{E_p}{E_s}\right)^{\frac{1}{4}}S_a\right]}\right\} \tag{14}$$

corresponding to a minimum (d_1), obtained for the minus (–) sign, and a maximum (d_2), obtained for the plus (+) sign, respectively. Values between these two extremes define the range of admissible pile diameters. It will be shown that d_1 is always larger than d_{in} in Equation 10a, and d_2 is always smaller than d_{kin} in Equation 7, that is the admissible range of pile diameters is narrower than that obtained by considering kinematic and inertial loads acting independently.

It should be noticed that if tip resistance is neglected (i.e., if $T_3 = 0$) the above result simplifies to the solution reported in Di Laora et al. (2013) and Mylonakis et al. (2014):

$$d_{1,2}=\frac{\varepsilon_y V_s^2}{a_s}\left\{1\mp\sqrt{1-\frac{24\alpha\rho_s a_s L}{q_A f_y \varepsilon_y SF}\left(\frac{E_s}{s_u}\right)\left[1+2\frac{q_A}{q_I}\left(\frac{\pi q_I}{\delta}\right)^{\frac{1}{4}}\left(\frac{a_s}{g}\right)\left(\frac{E_p}{E_s}\right)^{\frac{1}{4}}S_a\right]}\right\} \tag{15}$$

RESULTS

Figure 4 depicts some general trends based on the above results in terms of pile diameter versus soil shear wave propagation velocity. Diameters lying inside the hatched zone defined by Equation 14 are admissible, whereas those lying outside this zone are not. Evidently,

upper and lower bounds are sensitive to the value of V_S leading to a wider range of admissible diameters for stiffer soils. The curves for purely kinematic and purely inertial action (shown by continuous curves) in Equations 7 and 10a bound the admissible range from above and below, respectively, suggesting that kinematic and inertial moments interact detrimentally for pile safety. While this effect is exaggerated because of the assumption of simultaneous maxima in kinematic and inertial responses (Equation 12), an analogous pattern would be obtained for any linear combination of individual moments involving arbitrary positive weight factors e_{kin} and e_{in}. Interestingly, there always exists a minimum soil shear wave velocity for which the admissible range collapses to a single point corresponding to a unique admissible diameter (i.e., $d_1 = d_2$). This diameter can be obtained by eliminating the term in square root in Equation 14, to get

$$d_1 = d_2 = \frac{\varepsilon_y V_s^2}{a_s}\left(1 - T_3\right) \tag{16}$$

which, for zero tip contribution, is equal to exactly one half of that obtained for kinematic action alone under zero axial load (Equation 8). It is noteworthy that this diameter is independent of pile Young's modulus and wall thickness. The specific diameter is associated with a soil wave propagation velocity which will be referred in the ensuing to as "critical." This velocity may be derived by setting the term under the square root in Equation 14 equal to zero and solving for E_s. For zero tip contribution one gets:

$$V_{s,crit} = \left(\frac{E_p}{\rho_s}\right)^{\frac{1}{2}} \left[\frac{2\dfrac{q_A}{q_1}\left(\dfrac{\pi q_1}{3\delta}\right)^{\frac{1}{4}} \dfrac{a_s}{g} S_a}{\dfrac{q_A \varepsilon_y^2 SF}{24\alpha}\left(\dfrac{E_s}{s_u}\right)\left(\dfrac{E_p}{a_s \rho_s L}\right) - 1} \right]^2 \tag{17}$$

Evidently, for shear wave velocities smaller than critical, no real-valued pile diameters can be predicted from Equation 15, which suggests that the pile head cannot stay elastic under the prescribed free-field surface acceleration a_s.

With reference to a hollow steel pile, admissible diameters predicted by Equation 15 are plotted in Figure 5 as a function of V_S for different values of surface seismic acceleration (a_s/g) and pile length L. The detrimental effect resulting from the particular load combination becomes gradually more pronounced with increasing pile length and seismic acceleration,

due to the higher inertial loads. Note that for piles in very soft soil with V_S < 50 m/s, such as peat, the maximum pile diameter may be less than 1 m.

SIZE LIMITATION FOR STEEL PILES IN SOILS WITH STIFFNESS VARYING PROPORTIONALLY WITH DEPTH

For piles embedded in normally consolidated clay, a more realistic assumption is to consider soil stiffness varying proportionally with depth (i.e., Muir Wood 2004).

$$E(z) = \overline{E}_s \cdot z \tag{18}$$

$\overline{E}_s$ being the gradient of soil Young's modulus with respect to depth, z. Following Di Laora and Mandolini (2011), the kinematic moment atop a fixed-head pile in a soil having a stiffness variation with depth described by Equation 18, may be estimated from the following approximate equation:

$$M_{kin} = 1.36 a_s \rho_s \left(\frac{E_p}{\overline{E}_s} I_p \right)^{\frac{4}{5}} (1 + \nu_s) \tag{19}$$

In the above expression, soil mass density ρ_s has been considered constant – a reasonable assumption since density varies with depth at a much smaller rate than stiffness. Considering a hollow pile of thickness t, Equation 19 can be cast in the equivalent form:

$$M_{kin} = 0.185 a_s \rho_s \left(\frac{q_l E_p}{\overline{E}_s} \right)^{\frac{4}{5}} d^{\frac{16}{5}} \tag{20}$$

where ν_s = 0.5 has been assumed. Equations 19 and 20 reveal that the effect of pile diameter on maximum kinematic bending moment is less pronounced than in homogeneous soil, as the corresponding exponent is 3.2 (= 16/5) instead of 4, due to the proportionality of pile bending moment on I_p in Equation 2. This can be explained considering that an increase in pile diameter forces a larger portion of progressively stiffer soil (experiencing smaller curvatures) to induce kinematic bending at the pile head (Di Laora and Rovithis 2015).

Despite that, the power of 3.2 still exceeds the corresponding one for capacity 3 (see Equation 3), this minor difference is unlikely to generate a significant size constraint, as demonstrated below.

The inertial moment at the pile head may be calculated according to the formula provided by Reese and Matlock (1956; see also Karatzia and Mylonakis 2012, 2016) based on Winkler considerations, which can be expressed using the notation adopted in this paper as:

$$M_{in} = 0.93 \frac{S_a P_p a_s}{g} \left(\frac{q_I E_p I_p}{\delta \bar{E}_s} \right)^{\frac{1}{5}} \tag{21}$$

Expressing I_p in terms of d and P_p through Equation 4, the moment demand takes the form:

$$M_{in} = 1.6 \frac{S_a L \alpha s_u}{FS} \left(\frac{a_s}{g} \right) \left(\frac{q_I E_p}{\delta \bar{E}_s} \right)^{\frac{1}{5}} d^{\frac{9}{5}} \tag{22}$$

Note that in this case s_u indicates the undrained shear strength at a depth of a half pile length ($z = L/2$) to account for the linear increase in soil strength with depth. The above equation reveals that pile diameter exerts a weaker effect on inertial moment compared to the homogeneous soil case, with a power dependence on d of 1.8 (= 9/5) instead of 2 (since P_p is proportional to d) in Equation 9.

Equating seismic moment demand from Equations 20 and 22 with section capacity in Equation 3 and making use of Equation 4 for inertial load, the following dimensionless equation for the pile size is obtained:

$$0.185 \left(\frac{q_I E_p}{\bar{E}_s L} \right)^{\frac{4}{5}} \left(\frac{d}{L} \right)^{\frac{16}{5}} - \frac{\pi}{64} \left(\frac{q_I E_p \varepsilon_y}{a_s \rho_s L} \right) \left(\frac{d}{L} \right)^3 + \frac{\pi}{16} \frac{q_I \alpha s_u}{q_A FS a_s \rho_s L} \left(\frac{d}{L} \right)^2 + 1.6 \frac{S_a \alpha s_u}{FS \gamma L} \left(\frac{q_I E_p}{\delta \bar{E}_s L} \right)^{\frac{1}{5}} \left(\frac{d}{L} \right)^{\frac{9}{5}} = 0 \tag{23}$$

Due to the intrinsically non-integer nature of the exponents, no exact solutions for the pile diameter are possible from Equation 23. As a first approximation, setting the powers 16/5 and 9/5 equal to 3 and 2, respectively, the equation provides the non-trivial root:

$$d \cong \frac{\alpha s_u}{FS \gamma} \frac{1.6 S_a \left(\frac{q_I E_p}{\delta \bar{E}_s L} \right)^{\frac{1}{5}} + \frac{\pi}{16} \frac{q_I}{q_A a_s / g}}{0.185 \left(\frac{q_I E_p}{\bar{E}_s L} \right)^{\frac{4}{5}} - \frac{\pi}{64} \left(\frac{q_I E_p \varepsilon_y}{a_s \rho_s L} \right)} \tag{24}$$

which corresponds to a minimum diameter to withstand combined inertial and kinematic action. It is noteworthy that the above approximate analysis reveals a lack of a maximum

diameter requirement for the specific conditions. A more accurate, iterative solution to Equation 23 is outlined in the Appendix.

Inspecting Equations 20 and 22, two differences over the corresponding expressions for homogeneous soil can be identified:

1. Size limitations in terms of a minimum diameter are more critical, as inertial moment increases with diameter at a smaller rate than in homogeneous soil;
2. The maximum admissible diameter due to kinematic action is less important, since kinematic head bending increases with pile diameter almost with the same power (16/5 = 3.2), as does section Capacity 3.

These observations are evident in Figure 6, where the ranges of admissible diameters are compared for the cases of homogeneous and inhomogeneous soil. As can be noticed, for the latter case and beyond a certain diameter, the demand to capacity ratio is nearly constant. However, this does not suggest an overall weaker influence of kinematic interaction on size limits, as the minimum diameter is indeed affected by kinematic demand. In addition, it can be noticed that kinematic demand is higher than inertial demand even for relatively small diameters.

The role of pile size is further explored in Figure 7, which depicts the bounds of the admissible diameter regions for different values of the governing problem variables. As anticipated, no maximum diameter exists from a practical standpoint, so that the upper bound consists of a nearly vertical line in $\bar{E}_S$-d space. Pile size limitation thus reduces to a minimum diameter, which increases with soil resistance because of the larger mass carried by the pile assuming a constant value of FS. Figure 7a shows the role of design acceleration on pile size. Understandably, the admissible region shrinks with increasing (a_s/g), as the specific parameter affects both inertial and kinematic loading, and moves towards larger diameters. A similar effect is observed in Figure 7b, which depicts limit diameters as a function of normalized spectral acceleration. Compared to the previous case, the left bound remains steady as kinematic moments are not affected by the specific parameter. It is noted that for moderate to strong seismicity (a_s/g = 0.25–0.35) and common values of spectral amplification (S_a = 2.5), rigidly capped piles in soft clay require very high diameters (on the order of 2 meters) to resist seismic loads without yielding at the top. This may explain the large number of failures at the pile head observed in post-earthquake investigations (Mizuno

1987). Figures 7c and 7d illustrate the role of section capacity. Figure 7c shows that reducing the wall thickness may significantly narrow the admissible region, whereas material strength (Figure 7d) seems to be of minor importance. Figure 7e investigates the role of pile length on the admissible diameter. Since inertial loads are taken proportional to pile length L and due to the wide range of possible pile lengths, this parameter has a strong effect in controlling the minimum admissible pile diameter.

If a preliminary design carried out considering only axial bearing capacity does not satisfy seismic structural requirements, a common solution is to decrease the weight carried by the piles, thereby increasing the safety factor *FS*. The influence of *FS* on pile seismic performance is illustrated in Figure 7f, where the minimum diameter clearly decreases with increasing *FS*. It is worth noting that *FS* exerts an influence similar to that of spectral amplification S_a, the difference being that *FS* also affects the pile axial force whereas S_a does not. Given the low level of axial pile stress relative to section capacity, the two parameters have a similar role in restricting d. Nevertheless, it should be kept in mind that increasing the safety factor against axial bearing capacity leads to an increase in foundation cost over the original design. Studying cost aspects of piling lies beyond the scope of this work.

SIZE LIMITATIONS FOR CONCRETE PILES

The behavior of concrete piles is fundamentally different from that of steel piles, as the moment of inertia of a concrete cross section is typically higher and the material has negligible tensile strength. The impact of these differences on pile size limitations is examined below.

With reference to a cylindrical concrete pile, the section moment capacity may be estimated through the simplified formula[1] (Cosenza et al. 2011):

$$M_u = M_{u,c} + M_{u,s} = \frac{2}{3}\left(\frac{d}{2}\right)^3 \sin^3\theta f'_{ck} + \frac{2}{\pi}\left(\frac{d}{2} - c\right) A_s \sin\theta f_{yk} \tag{25}$$

where $M_{u,c}$ and $M_{u,s}$ denote, respectively, the relative contributions of concrete and steel, $f'_{ck} = 0.9\, f_{ck}$, the latter being the compressive strength of concrete, f_{yk} is the yield strength of steel reinforcement, and c is the thickness of the concrete cover. θ is a characteristic angle which can be derived from the solution of the transcendental equation:

[1] Due to a clerical error, a coefficient of 4/3 is reported in the original work instead of the correct 2/3 in Equation 25.

$$2\theta(1+2\omega)-\sin 2\theta-2\pi(\omega+\nu_k)=0 \tag{26}$$

where $\omega = A_s f_{yk} / (A_c f'_{ck})$ is the mechanical percentage of reinforcement and $\nu_k = W_p / (A_c f'_{ck})$ is the familiar dimensionless axial force parameter. θ can be easily derived from Equation 26 by using an iterative procedure analogous to the one described in the Appendix for the limit diameters, starting from an initial estimate $\theta = \pi/2$. As a simpler alternative, the trigonometric term $sin2\theta$ can be well approximated by the parabola $(16/\pi^2)\ \theta(\pi/2-\theta)$, for $\theta \leq \pi/2$, to transform the original transcendental expression into the second-order algebraic equation:

$$\frac{16}{\pi^2}\theta^2+2\left(1+2\omega-\frac{4}{\pi}\right)\theta-2\pi(\omega+\nu_k)=0 \tag{27}$$

which admits the positive root:

$$\theta=\left(\frac{\pi}{4}\right)^2\left(1+2\omega-\frac{4}{\pi}\right)\left[-1+\sqrt{1+\frac{32}{\pi}\frac{\omega+\nu_k}{(1+2\omega-4/\pi)^2}}\right] \tag{28}$$

A comparison between an exact numerical solution of Equation 26 and the approximate analytical solution in Equation 28 depicted in Figure 8, highlights the satisfactory performance of the closed-form solution.

By means of the above results, the ratio of moment capacities of steel and concrete cross sections may be calculated in closed form, as reported in Figure 9 for different values of reinforcement ratio (or wall thickness ratio) and axial load. It is observed that concrete sections possess lower capacity than steel ones, and this becomes more pronounced for higher values of reinforcement ratio A_s/A_c (assumed here to be equal to the wall thickness t/d). In addition, an increase in axial load lowers the capacity ratio, since the axial force may have a beneficial effect for a concrete section whereas it is always detrimental for a steel one.

In the same spirit as before, critical diameters may be assessed by equating capacity, given by Equation 25 and demand obtained by summing up the contributions of kinematic and inertial interaction (for $q_I = 1$), as shown earlier.

Numerical results for homogeneous soil are reported in Figure 10, where limit diameters are calculated for solid cylindrical concrete piles in $V_S - d$ plane, as functions of other salient problem parameters. Compared to the steel piles in Figure 5, the range of admissible diameters is smaller (see, e.g., curves for L = 50 m in Figures 10c and 5c obtained for a_s/g =

0.25 and $A_s/A_c = t/d$). Moreover, piles in high-seismicity areas ($a_s/g = 0.3$, Figure 10a) should possess large diameters which may even be prohibitive for construction reasons. The same behavior is noticeable for large values of spectral amplification ($S_a = 4$, Figure 10b), long piles carrying heavy loads ($L = 50$ m, Figure 10c) and small reinforcement ratios ($A_s/A_c = 1\%$, Figure 10d). Interesting trends are observed in Figures 10e and 10f where the limit diameters are calculated for different values of concrete and steel strength. Evidently, concrete strength has a negligible effect on the admissible regions, whereas steel quality is somewhat more important.

Concrete piles in soil with stiffness varying linearly with depth can be analyzed via Equation 25 for moment capacity, and Equations 20 and 22 (with $q_I = 1$) for kinematic and inertial moment demand, respectively. Numerical results are depicted in Figure 11. This case leads to the narrowest regions of admissible diameters compared to those examined earlier (see, e.g., curves for $S_a = 1$ in Figures 11b and 7b). As with hollow steel piles, maximum diameter in soil with stiffness varying proportionally with depth is not important from a practical viewpoint, since the curves tend to become nearly vertical at the left end of the graphs. Nevertheless, kinematic interaction plays a major role in controlling (increasing) the minimum diameter. Concrete and steel strengths are of minor importance, whereas seismicity (Figures 11a and 11b) and geometrical parameters (Figures 11c and 11d) have a considerable effect in establishing the minimum admissible diameter.

A comparison of the four cases examined herein is provided in Figure 12, where admissible regions are plotted for steel and concrete piles embedded in homogeneous and linear soil profiles. Curves corresponding to linearly varying soil stiffness are somewhat rotated with respect to the homogeneous case, because of the different effect of pile diameter on kinematic bending. As already demonstrated, maximum diameter is of concern only for homogeneous and very soft inhomogeneous soils, whereas in all other cases a minimum diameter is of the main concern. Very large diameters may be required due to the detrimental interplay of kinematic and inertial moment demands on the pile.

DISCUSSION

It has already been shown that for homogeneous soil kinematic interaction provides a minimum admissible pile diameter, while inertial interaction leads to a maximum one. As

these actions interact detrimentally, the range is reduced for simultaneous action over the hypothetical case of kinematic and inertial loads acting independently.

In very soft deposits, if soil stiffness close to the surface is assumed to be nearly constant with depth (which is typical in natural clays) kinematic interaction has a dominant influence, resulting to small maximum admissible diameters. In these cases inertial interaction, while generating smaller bending demands compared to kinematic one, may have an important effect in reducing the maximum admissible diameter obtained for sole kinematic loading. Under the assumptions adopted in this work, pile length has a remarkable role in reducing the admissible pile diameter and increasing the critical soil stiffness below which no pile diameter is admissible, so that in some cases modifications in foundation design may be needed.

For stiffer soils and/or linearly varying stiffness with depth, the pile size limitations essentially reduce to a minimum diameter. In several cases, safety factors commonly used in classical geotechnical design for axial bearing capacity do not guarantee structural safety under seismic action. To address the problem, a possible solution would be to increase the number of piles, thus increasing the safety factor against gravitational action. An alternative choice would be to increase the capacity of the pile cross section by increasing the wall thickness or the reinforcement. On the other hand, increasing material strength will not improve pile performance to an appreciable extent. Overall, it can be concluded that geotechnical and geometrical material properties as well as seismicity parameters play a more important role over structural material properties in controlling pile design.

EFFECT OF PILE DIAMETER ON SOIL-PILE CONTACT STRESSES

With reference to nonlinear effects, an important question is whether soil can force a large-diameter pile to yield without itself reaching an ultimate limit pressure against the pile shaft. An analytical investigation of this possibility has been included in this work as an online Appendix. A summary is provided below. For simplicity, only homogeneous soil and harmonic ground excitation are considered, although the analysis can be extended to more general conditions in a straightforward manner.

According to Winkler theory, the pile-soil interaction force per unit pile length at any depth is:

$$p = -k\left(y - u_s\right) \tag{29}$$

where k is the modulus of subgrade reaction, measured in units of pressure, y is pile deflection and u_s is the free-field soil displacement at the same depth. Moreover, any stress component σ_{ij} acting on the pile periphery can be expressed as:

$$\sigma_{ij} = \chi_{ij} p / d \tag{30}$$

χ_{ij} being a dimensionless constant dependent on stress component, location along the periphery and soil Poisson's ratio (Karatzia et al 2014). Considering harmonic excitation, it can be shown (see the online Appendix) that Equation 30) takes the form:

$$\sigma_{ij} = 2k\chi_{ij} \frac{\left(\frac{\omega}{\lambda V_s}\right)^2}{\left(\frac{\omega}{\lambda V_s}\right)^4 + 4} \varepsilon_y \cos\left(\frac{\omega z}{V_s}\right) \tag{31}$$

where ($\omega/\lambda V_S$) can be interpreted as a dimensionless frequency analogous to the familiar dimensionless frequency ($\omega d/V_S$; Anoyatis et al. 2013), and ε_y here stands for a characteristic soil yield strain.

The result in Equation 31 indicates that the pile-soil contact stresses σ_{ij} in a homogeneous soil layer are zero both for very small and very large diameters. The former limit is anticipated as a small diameter d corresponds to a low dimensionless frequency ($\omega/\lambda V_S$; recall that is proportional to $d^{-1/4}$), thereby the pile follows the soil motion (i.e., $\Psi = 1$, in Equation 1. The second limit is also anticipated on the basis of Equation 30, which reflects the distribution of the interaction force per unit pile length p over a wider area leading to a reduction in contact stresses in proportion to ($1/d$).

The above double asymptotic behavior elucidates the weak dependence of pile-soil contact stresses on pile diameter, therefore the analytical developments presented in this article are applicable to both small-diameter and large-diameter piles. It must be kept in mind, however, that this investigation is strictly applicable to kinematic loading and should not be used for interpreting pile-soil contact stresses due to loads applied at the pile head.

EFFECT OF SOIL NONLINEARITY

With reference to the importance of nonlinear effects in the soil, the following are worthy of note: (1) material nonlinearity in the free field may have a dominant effect in controlling the value of shear wave propagation velocity V_S and soil acceleration a_s at the pile head; (2)

as evident from Equation 31, soil stiffness has a minor effect in controlling the magnitude of kinematically induced stresses at the pile-soil interface. Accordingly, kinematically induced nonlinearity in the soil is typically minor, which can be understood given the small displacement mismatch between pile and soil under such conditions (see also Turner et al. 2015, Martinelli et al. 2016); (3) Equations 9 and 22 indicate that inertial bending moment at the pile head depends, respectively, on the fourth and fifth root of soil stiffness in homogeneous and inhomogeneous soil, so moment is not sensitive to stiffness degradation due to soil material nonlinearity. (This is in contrast to pile head stiffness and associated displacements, which are sensitive to soil stiffness.)

In summary, whereas soil material nonlinearity in the free field may be dominant and should be considered when establishing the shear wave propagation velocity and acceleration profiles, additional nonlinearities due to kinematic and inertial soil-pile-structure interaction are typically minor and can be neglected for the purposes of the analyses reported in this work.

SAMPLE APPLICATION

A solid concrete cylindrical fixed-head bored pile carrying a vertical load of 700 kN is to be embedded in a deep, normally consolidated clay layer and needs to be designed against combined gravitational and seismic action under undrained conditions. The subsoil has a linear variation in both stiffness and undrained shear strength with depth, with $\overline{E}_s$ = 3 MPa/m and $\overline{s}_u$ = 4 kPa/m. Seismicity parameters are a_s/g = 0.25 and S_a = 2.5. Material properties are E_p = 30 GPa, f_{ck} = 25 MPa, f_{yk} = 450 MPa, ν_s = 0.5. An adhesion coefficient α = 2/3 is assumed for the undrained skin friction.

Ordinary design for gravitational loading allows infinite combinations of pile diameter and length for a given safety factor. For the purposes of this example, the following candidate solutions are considered:

1. L = 10 m, d = 2 m
2. L = 20 m, d = 1 m
3. L = 32 m, d = 0.5 m

all of which ensure a global safety factor FS of approximately 2.5 against gravitational loading.

By means of the equations provided in the paper (Equations 20, 22, 25, and 28) it is possible to design the pile against seismic action through the following six steps:

1. Consider a pair (L, d) based on a preliminary design against gravitational action.
2. Calculate the peak kinematic bending moment at the pile head from Equation 20.
3. Calculate the peak inertial bending moment at the pile head from Equation 22.
4. Superimpose the two moments for the overall bending action M_{tot} via Equation 12.
5. Determine the amount of steel reinforcement A_s that balances bending demand and capacity according to Equation 25. To this end, one has to assume a value of A_s, calculate v_d, ω and θ from Equation 28, and then moment capacity from Equation 25. Note that for design purposes, factored values must be used instead of characteristic strengths and demands. The procedure has to be repeated in an iterative manner by increasing/decreasing A_s until M_{tot} is matched.
6. Repeat Steps 2 to 5 for different pairs (L, d).

The results for the three pile configurations of this example are, assuming design strengths for steel and concrete to be, respectively, 0.87 (= 1/1.15) and 0.576 (= 0.85/1.5) times the corresponding characteristic values:

1. A_s = 405 cm^2 (A_s/A_c = 1.3 %, M_{kin} = 11234 kNm, M_{in} = 847 kNm)
2. A_s = 168 cm^2 (A_s/A_c = 2.13 %, M_{kin} = 1222 kNm, M_{in} = 973 kNm)
3. A_s = 159 cm^2 (A_s/A_c = 8.1 %, M_{kin} = 133 kNm, M_{in} = 716 kNm)

The sharp decrease in M_{kin} with decreasing pile diameter and the corresponding small variation in M_{in} are evident.

Configurations 1 and 2 are clearly acceptable, having a reinforcement ratio between 1 and 4%, which lie within the design limits specified by design codes, while the third one is unacceptable—both from a ductility and a construction viewpoint. Configuration 2 may be viewed as the preferred one, despite an increase in pile length over the first configuration, since it involves a lower diameter, about 50% the volume of excavated soil and concrete, and 40% the area of steel reinforcement as compared to configuration 1. Translating these figures

into cost depends on additional factors which lie beyond the scope of this work. As a final remark, the better overall performance of the smallest pile diameter in configuration 3 (which attracts the lowest kinematic bending) is worth noting.

CONCLUSIONS

The work at hand dealt with size limitations on piles in seismically prone areas, exploring the development of bending at pile head due to combined kinematic and inertial actions, which are of different nature and, thereby, are affected by pile size in a different manner. The study assumes that the pile is designed to remain elastic during earthquake shaking, as required by modern seismic codes, while the soil can be treated as a nonlinear material with its shear modulus decreasing with increasing level of shear strain in the free-field and in the vicinity of the pile. With reference to the pile head, which was assumed to be perfectly restrained against rotation, it was shown that: (a) kinematic interaction provides a maximum diameter beyond which the pile cannot resist seismic demand in an elastic manner, (b) inertial interaction provides a minimum corresponding diameter, and (c) the simultaneous presence of both actions leads to a narrower range of admissible diameters than the one obtained from the limits in (a) and (b). Exploring this range was the focus of the article both for steel and concrete piles, in soils of constant stiffness and stiffness varying proportionally with depth. The main conclusions of the study are summarized below:

1. The range of admissible diameters decreases with increasing design ground acceleration, spectral amplification, soil strength and pile length, whereas it increases with increasing soil stiffness, safety factor against gravitational loading and amount of reinforcement (or wall thickness). On the contrary, pile material strength has a minor effect in controlling pile size.

2. Concrete piles were found to be subjected to more severe size limitations due to the higher bending stiffness of the concrete pile cross section as well as the inability of the concrete material to carry tension.

3. For soft soils of constant stiffness with depth, kinematic interaction dominates seismic demand and the resulting pile diameter is over-bounded by a critical value which may be quite small (less than 1 m) and, therefore, affect design. In this case the addition of piles or an increase in pile length does not improve safety because these changes do not affect kinematic moments. Conversely, in stiffer soils,

inertial interaction is prominent due to the heavier load carried by the pile under a constant factor of safety against gravitational action and this may lead to a larger minimum diameter.

4. Soils with stiffness increasing proportionally with depth enforce only a lower bound on pile diameter, which may be rather large (above 2 m). The absence of an upper limit is noticeable despite kinematic demand being generally large.

5. There is always a critical soil shear wave velocity (or stiffness gradient) below which no pile diameter is admissible for a given design ground acceleration. Below this threshold a fixed-head pile cannot stay elastic regardless of diameter or material strength. It should be noted that in the extreme case where $V_S = 0$ (e.g., a pile in water), no diameter is apparently admissible. This behavior should not be viewed as paradoxical, since in that case a_s would also be zero. Exploring the interplay between V_S and a_s lies beyond the scope of this study.

6. Pile-soil contact stresses due to kinematic interaction are not expected to be important at low frequencies and do not induce additional nonlinearities in the soil near the pile shaft.

It must be emphasized that the work at hand focus on pile size limitations due to seismic action. The complementary topic of the beneficial role of large-diameter piles in reducing structural seismic forces by filtering out the high frequency components of the seismic motion through kinematic interaction may be of importance and is addressed elsewhere (Di Laora and de Sanctis 2013). Also, some of the conclusions may require revision in presence of strong nonlinearities in the soil and the pile (see Taciroglu et al. 2006), such as those associated with soil liquefaction and pile buckling. As a final remark, it is fair to mention that while no sensitivity analyses have been undertaken to quantify the importance of some of the approximations involved (notably the superposition of kinematic and inertial bending moments), the results are generally conservative. There is also some evidence (Di Laora 2010) that for the common situation where the structural period is lower than the natural period of the foundation input motion, kinematic and inertial effects in terms of pile bending moments are more or less in phase, so the summation of maxima employed in this work is justified.

APPENDIX

Please refer to the online version of this paper to access the supplementary material in the Appendix.

NOMENCLATURE

LATIN SYMBOLS

$(1/R)_p$	Pile (head) curvature
$(1/R)_s$	Free-field soil curvature (at surface)
A	Pile cross-sectional area
A_c	Area of concrete in pile cross section
A_s	Area of steel reinforcement in the cross section
a_0	(= $\omega/\lambda V_S$, $\omega d/V_S$) dimensionless frequencies
a_s	Free-field soil acceleration (at surface)
c	Thickness of concrete cover
d	Pile diameter
d_{in}	Minimum allowable diameter due to inertial action
d_{kin}	Maximum allowable diameter due to kinematic action
E_p	Pile Young's modulus
E_s, $E_s(z)$	Soil Young's modulus
$\bar{E}_s$	Gradient of soil Young's modulus with depth
e_{in}, e_{kin}	Correlation coefficients
f_{ck}	Characteristic compressive strength of concrete
f'_{ck}	Conventional compressive strength of concrete
f_{yk}	Yield strength of reinforcement
f_y	Uniaxial yield stress of steel
g	Acceleration of gravity
k	Modulus of subgrade reaction (units of F/L^2)
I_p	Pile cross-sectional moment of inertia
L	Pile length
M_{head}^{kin}	Kinematic pile (head) bending moment
M_{tot}	Total moment demand
M_u	Cross-sectional moment capacity
$M_{u,c}$	Contribution of concrete to cross-sectional moment capacity
$M_{u,s}$	Contribution of reinforcement to cross-sectional moment capacity
M_y	Cross-sectional moment capacity of a steel pile
N_c	Pile tip bearing capacity factor
p	Soil reaction force per unit pile length (units of F/L)
q_A, q_I	Dimensionless geometric factors
P_p	Pile axial load under working conditions
S_a	Dimensionless spectral amplification
s_u	Undrained soil shear strength
T_1, T_2, T_3	Dimensionless pile tip bearing capacity coefficients
V_S	Shear wave propagation velocity in the soil
u_s	Free-field soil displacement
y	Pile deflection
z	Depth

GREEK SYMBOLS

α	Pile-soil adhesion coefficient
γ	Soil unit weight
δ	Winkler stiffness parameter
ε_y	Yield strain
θ	Characteristic angle
ν_s	Soil Poisson's ratio
ν_k	Dimensional pile axial force
ρ_s	Soil mass density
χ_{ij}	Dimensionless constant
Ψ	Soil-structure interaction dimensionless factor
ω	Mechanical percentage of reinforcement

REFERENCES

Anoyatis, G., Di Laora, R., Mandolini, A., and Mylonakis, G., 2013. Kinematic response of single piles for different boundary conditions: Analytical solutions and normalization schemes, *Soil Dynamics and Earthquake Engineering* **44**, 183–195.

Anoyatis, G., Mylonakis, G., and Lemnitzer, A., 2016. Soil reaction to lateral harmonic pile motion, *Soil Dynamics and Earthquake Engineering* **87**, 164–179.

Brandenberg, S. J., Boulanger, R. W., Kutter, B. L., and Chang, D., 2005. Behavior of pile foundations in laterally spreading ground during centrifuge tests, *Journal of Geotechnical and Geoenvironmental Engineering* **131**, No. 11, 1378–1391.

Castelli, F., and Maugeri, M., 2009. Simplified approach for the seismic response of a pile foundation, *Journal of Geotechnical and Geoenvironmental Engineering* **135**, 1440–1451.

Cosenza, E., Galasso, C., and Maddaloni, G., 2011. A simplified method for flexural capacity assessment of circular RC cross sections, *Engineering Structures* **33**, 942–946.

de Sanctis, L., Maiorano, R. M. S., and Aversa, S., 2010. A method for assessing bending moments at the pile head, *Earthquake Engng Struct. Dyn* **39**, 375–397.

Dezi, F., Carbonari, S., and Leoni, G., 2010. Kinematic bending moments in pile foundations, *Soil Dyn. Earthquake Engng* **30**, No. 3, 119–132.

Di Laora, R., 2010. Phase lag between kinematic and inertial interaction, *XXV EYGEC*, Brno, Czech Republic.

Di Laora, R., and Mandolini, A., 2011. Some Remarks about Eurocode and Italian code about piled foundations in seismic area*, ERTC-12 Workshop on Evaluation of EC8*, Athens, Greece.

Di Laora, R., Mandolini, A., and Mylonakis, G., 2012. Insight on kinematic bending of flexible piles in layered soil, *Soil Dynamics and Earthquake Engineering* **43,** 309–322.

Di Laora, R., Mandolini, A., and Mylonakis, G., 2012. Selection criteria for pile diameter in seismic areas, *2nd International Conference on Performance-Based Design in Geotechnical Engineering*, Taormina, Italy.

Di Laora, R., and de Sanctis, L., 2013. Piles-induced filtering effect on the foundation input motion, *Soil Dynamics and Earthquake Engineering* **46**, 52–63.

Di Laora, R., Mylonakis, G., and Mandolini, A., 2013. Pile-head kinematic bending in layered soil, *Earthquake Engineering and Structural Dynamics* **42**, 319–337.

Di Laora, R., and Rovithis, E., 2015. Kinematic bending of fixed-head piles in nonhomogeneous soil, *J. Geotech. Geoenviron. Eng.***141**, No. 4, 04014126.

Dobry, R., Vicente, E., O'Rourke, M., and Roesset, M., 1982. Horizontal stiffness and damping of single piles, *Journal of Geotechnical and Geoenvironmental Engineering* **108**, 439–759.

Gajan, S., and Kutter, B. L., 2008. Capacity, settlement, and energy dissipation of shallow footings subjected to rocking, *Journal of Geotechnical and Geoenvironmental Engineering* **134**, 1129–1141.

Gazetas, G., Anastasopoulos, I., Adamidis, O., and Kontoroupi, T., 2013. Nonlinear rocking stiffness of foundations, *Soil Dynamics and Earthquake Engineering* **47**, 83–91.

Kavvadas, M., and Gazetas, G., 1993. Kinematic seismic response and bending of free-head piles in layered soil, *Géotechnique* **43,** 207–222.

Kaynia, A. M., and Mahzooni, S., 1996. Forces in pile foundations under seismic loading, *Journal of Engineering Mechanics* **122**, 46–53.

Karatzia, X., and Mylonakis, G., 2016. Horizontal Stiffness and Damping of Piles in Inhomogeneous soil, *J. Geotech. Geoenv. Eng., ASCE* (in press, DOI: 10.1061/(ASCE)GT.1943-5606.0001621).

Karatzia, X., Papastylianou, P., and Mylonakis, G., 2014. Horizontal soil reaction of a cylindrical pile segment with a soft zone, *Journal of Engineering Mechanics*, ASCE, **140**, 04014077.

Karatzia, X., and Mylonakis, G., 2012. Horizontal response of piles in inhomogeneous soil: Simple analysis, *2nd International Conference on Performance-Based Design in Geotechnical Engineering*, Taormina, Italy.

Maiorano, R. M. S., de Sanctis, L., Aversa, S., and Mandolini, A., 2009. Kinematic response analysis of piled foundations under seismic excitations, *Can. Geotech. J*. **46,** 571–584.

Margason, E., 1975. *Pile Bending during Earthquakes*, Lecture, 6 March 1975, ASCE/UC Berkeley Seminar on Design Construction and Performance of Deep Foundations.

Margason, E., and Holloway, D. M., 1977. Pile bending during earthquakes, *Proc. 6th World Conference on Earthquake Engng*, Sarita Prakashan, Meerut, India, 1690–1696.

Martinelli, M., Burghignoli, A., and Callisto, L., 2016. Dynamic response of a pile embedded into a layered soil, *Soil Dynamics and Earthquake Engineering* **87**, 16–28.

Millen, M., 2016. Integrated Performance Based Design of Building Foundation Systems, Ph.D. Dissertation, University of Canterbury, Christchurch, New Zealand.

Mineiro, A. J. C., 1990. *Simplified Procedure for Evaluating Earthquake Loading on Piles*, De Mello Volume, Lisbon.

Mizuno, H., 1987. Pile damage during earthquakes in Japan, in *Dynamic Response of Pile Foundations* (T. Nogami, Editor), ASCE Special Publication No. 11, 53–78.

Muir Wood, D., 2004. *Geotechnical Modelling*, Spon Press, London.

Mylonakis, G., 2001. Simplified model for seismic pile bending at soil layer interfaces, *Soils and Foundations* **41**, 47–58.

Mylonakis, G., Di Laora, R., and Mandolini, A., 2014. The role of pile diameter on earthquake-induced bending, *Theme Lecture, 15th European Conference on Earthquake Engineering*, Istanbul, 24–29 August 2014, 533–556.

Nikolaou, A., Mylonakis, G., Gazetas, G., and Tazoh, T., 2001. Kinematic pile bending during earthquakes analysis and field measurements, *Géotechnique* **51**, 425–440.

Novak, M., Nogami, T., and Aboul-Ella, F., 1978. Dynamic soil reaction for plane strain case. *J. Engng Mech. Div.*, ASCE, **104**, 1024–1041.

Pender, M., 1993. Aseismic pile foundation design analysis, *Bulletin of the New Zealand National Society for Earthquake Engineering* **26**, 49–160.

Popov, E. P., 1976. *Mechanics of Materials,* 2nd Edition, Prentice-Hall, NJ.

Reese, L. C., and Matlock, M. M., 1956. Non dimensional solutions for laterally loaded piles with soil modulus assumed proportional to depth, *VIII Texas Conf. SMFE*, Spec. Publ. 29, University of Texas, Austin.

Roesset, J. M., 1980. The use of simple models in soil-structure interaction, *ASCE Specialty Conference*, Knoxville, TN, Civil Engineering and Nuclear Power, vol. 2.

Saitoh, M., 2005. Fixed-head pile bending by kinematic interaction and criteria for its minimization at optimal pile radius, *Journal of Geotechnical and Geoenvironmental Engineering* **131**, 1243–1251.

Sica, S., Mylonakis, G., and Simonelli, A. L., 2011. Transient kinematic pile bending in two-layer soil. *Soil Dyn. Earthquake Engng* **31**, 891–905.

Syngros, K., 2004. *Seismic response of piles and pile-supported bridge piers evaluated through case histories*. Ph.D. Thesis, City University of New York.

Taciroglu, E., Rha, C., and Wallace, J. W., 2006. A robust macroelement model for soil-pile interaction under cyclic loads, *J. Geotech. Geoenviron. Eng*. **132**, 1304–1314.

Turner, B.J., Brandenberg, S.J. and Stewart, J.P., 2015. Influence of kinematic SSI on foundation input motions for pile-supported bridges, *6ICEGE*, New Zealand, 2015.

Varun, V., Assimaki, D., and Shafieezadeh, A., 2013. Soil-pile-structure interaction simulations in liquefiable soils via dynamic macroelements: Formulation and validation, *Soil Dynamics and Earthquake Engineering* **47**, 92–107.

Viggiani, C., Mandolini, A. and Russo, G., 2012. *Piles and Pile Foundations*, Spon Press, Taylor and Francis Ltd, London and New York.

Figure 1. Kinematic and inertial loading and associated bending profile of pile foundations.

Figure 2. Soil profiles (a, b) and pile sections (I, II) considered in the study.

Figure 3. Kinematic and inertial bending moments over corresponding capacity as function of pile diameter.

Figure 4. Range of admissible and inadmissible diameters for different types of loading. For inertial and gravitational loads points above curves are admissible and vice versa. The opposite is true for the curve involving solely kinematic action.

Figure 5. Admissible pile diameters against soil shear wave velocity (E_s/s_u = 500, $f_{yk,s}$ = 275 MPa, E_p = 210 GPa, ν_s = 0.5, ρ_s = 1.7 Mg/m^3, S_a = 2.5, F_S = 3, t/d = 0.015, α = 0.7, δ = 1.2, T_1 = 0). Continuous lines represent pure kinematic and inertial actions whereas dashed lines refer to the combined action.

Figure 6. Kinematic, inertial and combined moment vs. capacity for homogeneous and linear soil stiffness profile. In all graphs, a_s/g = 0.35, E_s/s_u = 500, $f_{yk,s}$ = 275 MPa, E_p = 210 GPa, ν_s = 0.5, ρ_s = 1.7 Mg/m^3, S_a = 2.5, FS = 3, t/d = 0.015, α = 0.5, L = 15 m, $\bar{\mathbf{E}}_\mathbf{s}$ = 2 MPa/m, E_s = $\bar{\mathbf{E}}_\mathbf{s}$ L/2 = 15 MPa.

Figure 7. Admissible pile diameters for a steel pile in soil with stiffness proportional to depth. In all graphs, except specifically otherwise stated, a_s/g = 0.25, E_s/s_u = 500, $f_{yk,s}$ = 355 MPa, E_p = 210 GPa, ν_s = 0.5, ρ_s = 1.7 Mg/m^3, S_a = 2.5, FS = 3, t/d = 0.015, α = 0.5, L = 30 m.

Figure 8. Comparison between the exact values of θ (Equation 26) and the estimates provided by the approximate formula in Equation 28, for different values of reinforcement percentage.

Figure 9. Capacity ratio of steel over concrete section as a function of diameter for different values of the reinforcement ratio (or wall thickness ratio) and dimensionless axial load. (s_u = 60 kPa, α = 0.5, FS = 3, L = 20 m, f_{ck} = 25 MPa, f_{yk} = $f_{yk,s}$ = 450 MPa, = $N/(f'_{ck}\,\pi d^2/4)$ = $N/(f_{yk,s}\,q_I\,\pi d^2/4)$).

Figure 10. Admissible pile diameters for a concrete pile in homogeneous soil. In all graphs, except specifically otherwise stated, a_s/g = 0.25, E_s/s_u = 500, E_p = 30 GPa, ν_s = 0.5, ρ_s = 1.7 Mg/m^3, S_a = 2.5, FS = 3, A_s/A_c = 0.015, f_{ck} = 25 MPa, f_{yk} = 450 MPa, α = 0.5, L = 30 m.

Figure 11. Admissible pile diameters for a concrete pile in soil with stiffness proportional to depth. In all graphs, except specifically otherwise stated, a_s/g = 0.2, E_s/s_u = 500, E_p = 30 GPa, ν_s = 0.5, ρ_s = 1.7 Mg/m^3, S_a = 2.5, FS = 3, A_s/A_c = 0.015, f_{ck} = 25 MPa, f_{yk} = 450 MPa, α = 0.5, L = 30 m.

Figure 12. Steel and concrete piles in homogeneous or linear stiffness profile. In all graphs, a_s/g = 0.25, E_s/s_u = 500, $f_{yk,s}$ (steel) = f_{yk} (concrete reinforcement) = 450 MPa, f_{ck} = 25 MPa, E_p = 30 GPa or 210 GPa (for concrete and steel, respectively), ν_s = 0.5, ρ_s = 1.7 Mg/m^3, S_a = 2.5, FS = 3, t/d = A_s/A_c = 0.015, α = 0.5, L = 30 m.

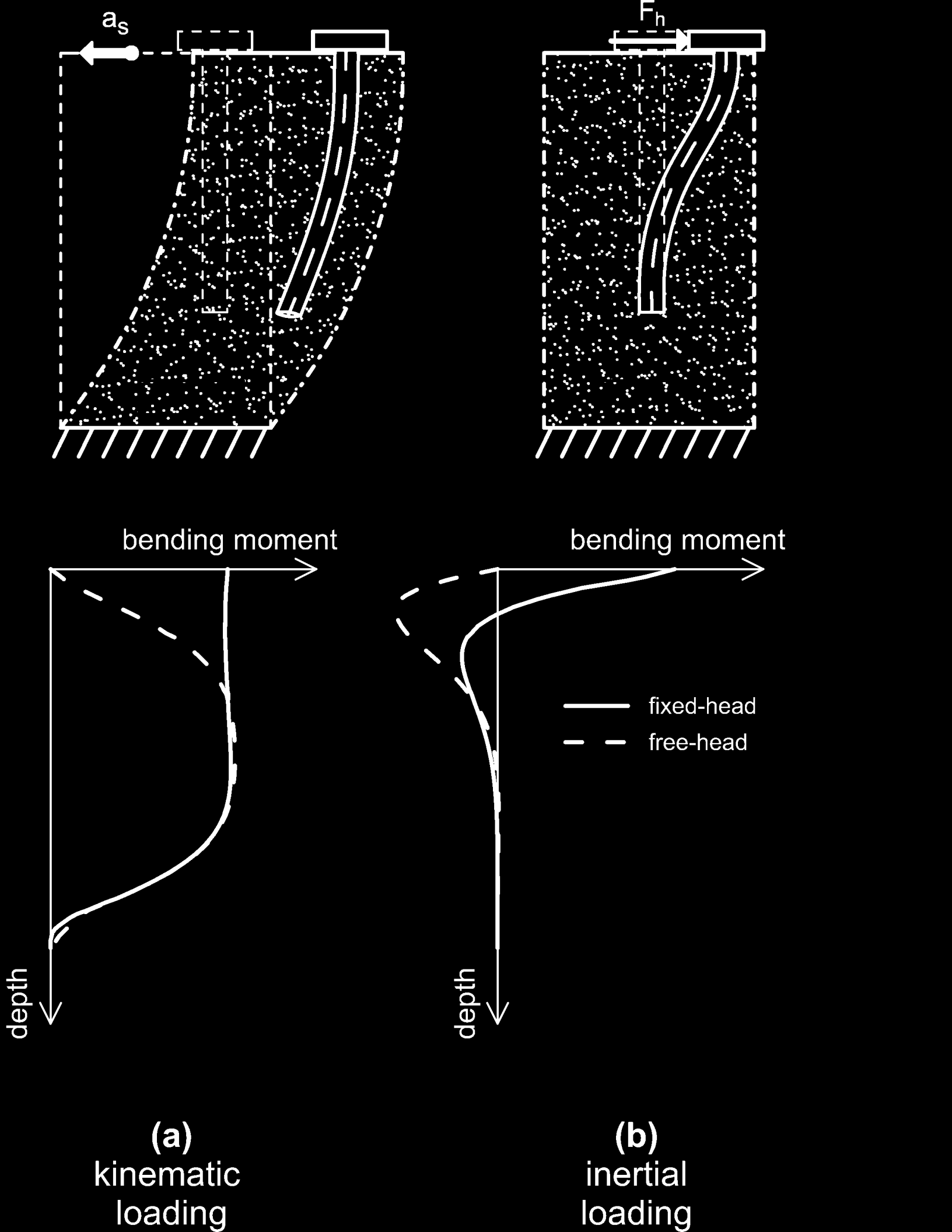
a_s
F_h
bending moment
bending moment
fixed-head
free-head
depth
depth
(a)
kinematic
loading
(b)
inertial
loading

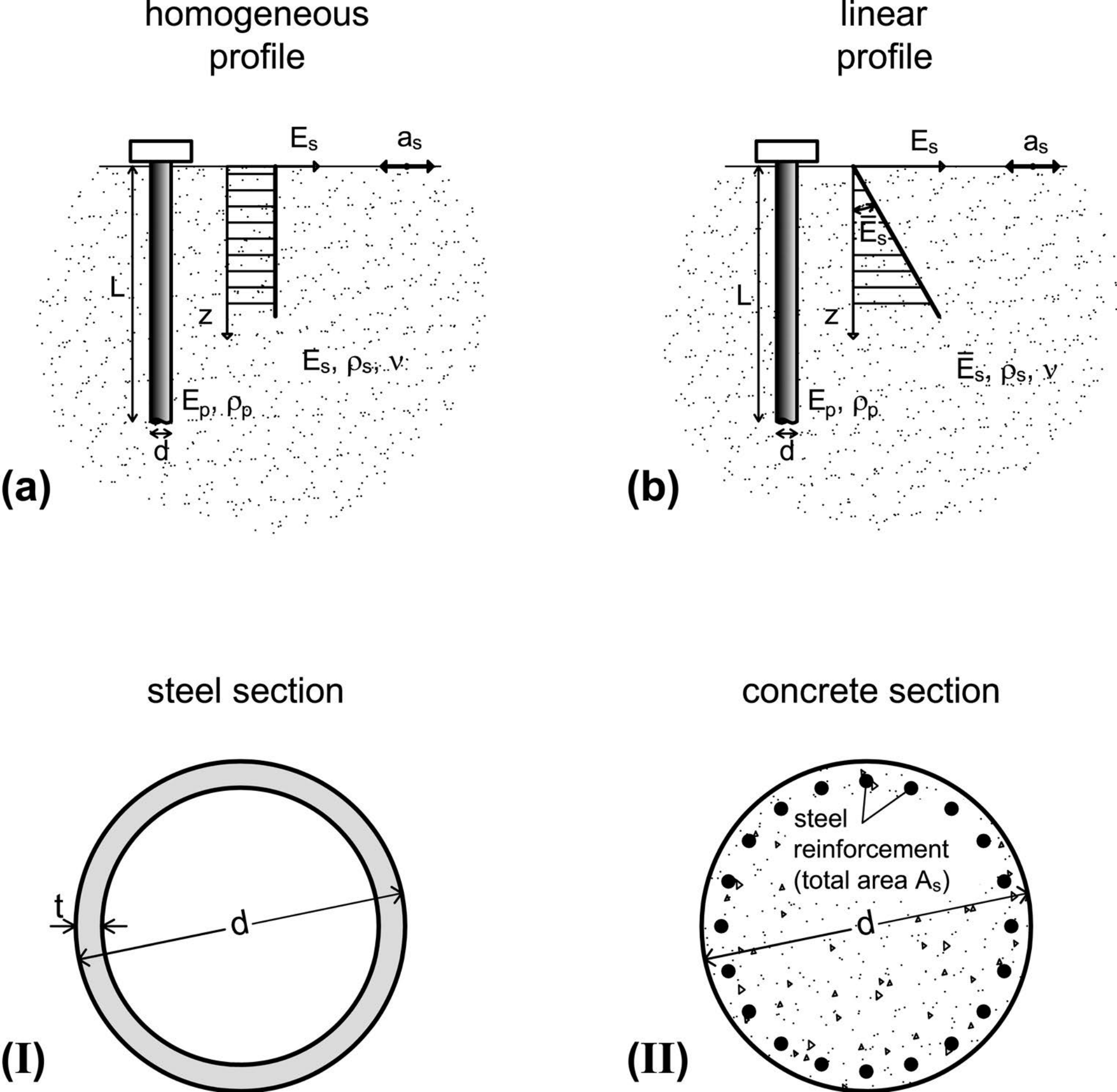
homogeneous
profile
linear
profile
E_s
a_s
L
z
E_s, ρ_s, ν
E_p, ρ_p
d
(a)
(b)
steel section
concrete section
t
d
steel
reinforcement
(total area A_s)
(I)
(II)

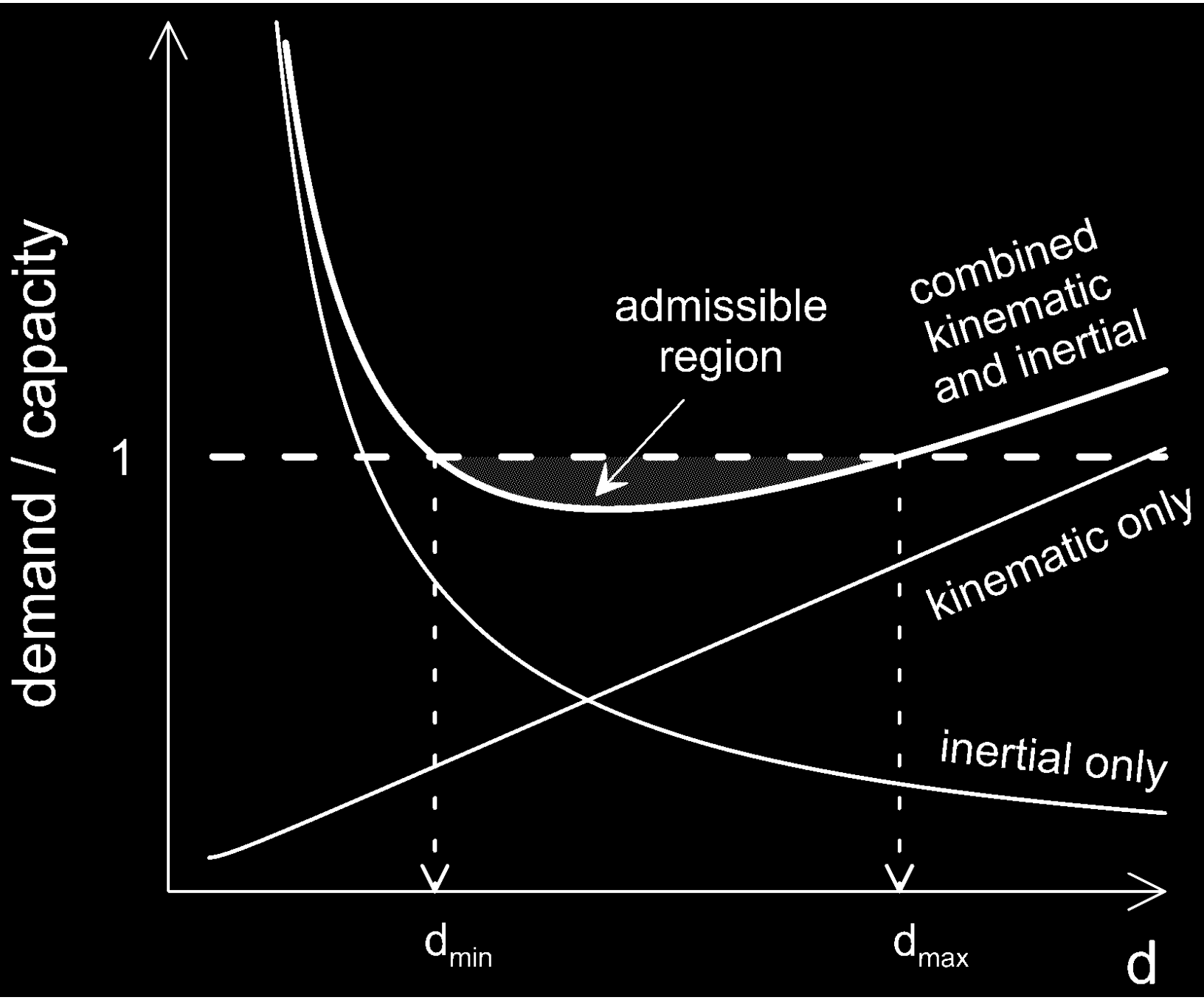
demand / capacity
1
admissible
region
combined
kinematic
and inertial
kinematic only
inertial only
d_{min}
d_{max}
d

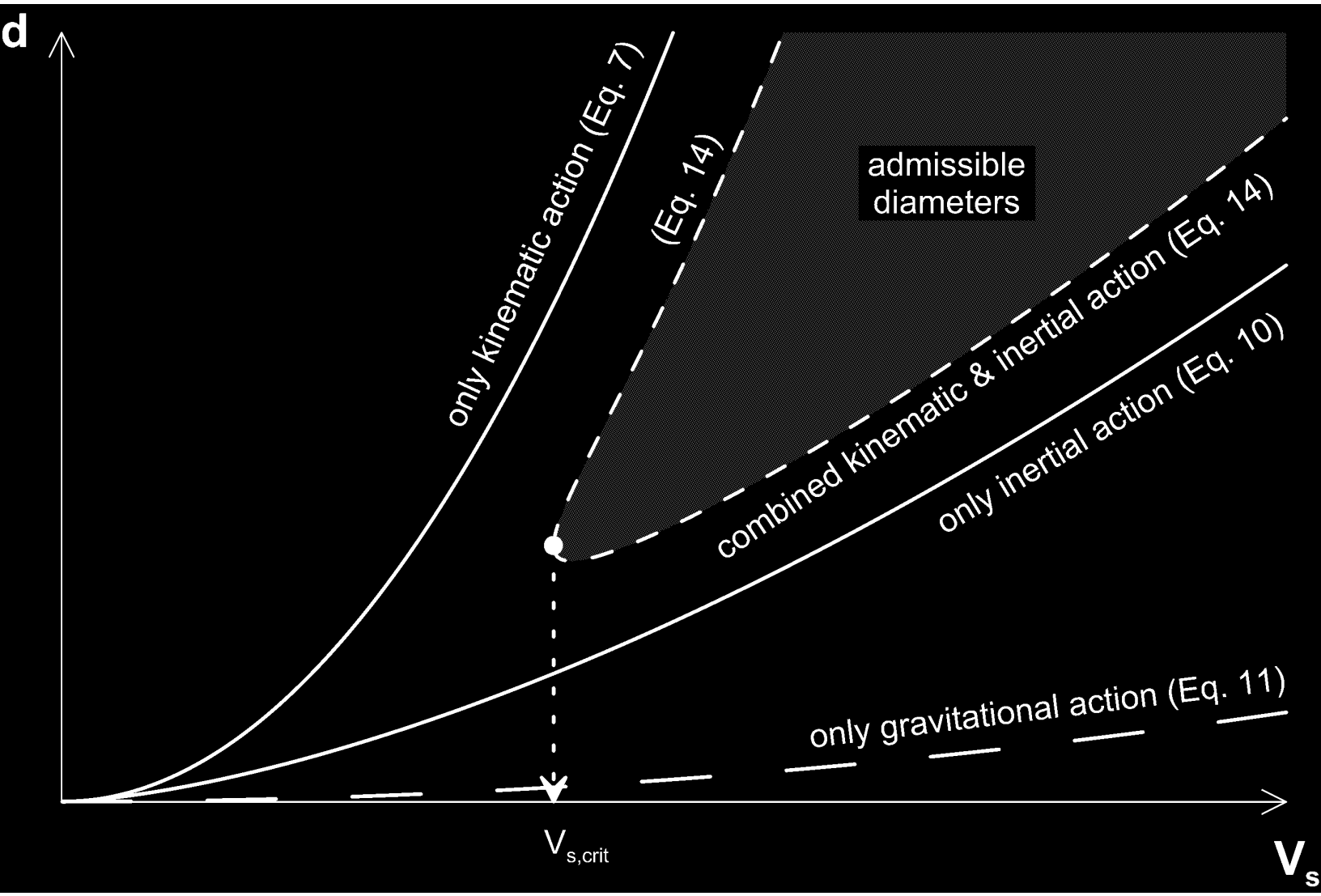
d
only kinematic action (Eq. 7)
(Eq. 14)
admissible
diameters
combined kinematic & inertial action (Eq. 14)
only inertial action (Eq. 10)
only gravitational action (Eq. 11)
$V_{s,crit}$
V_s

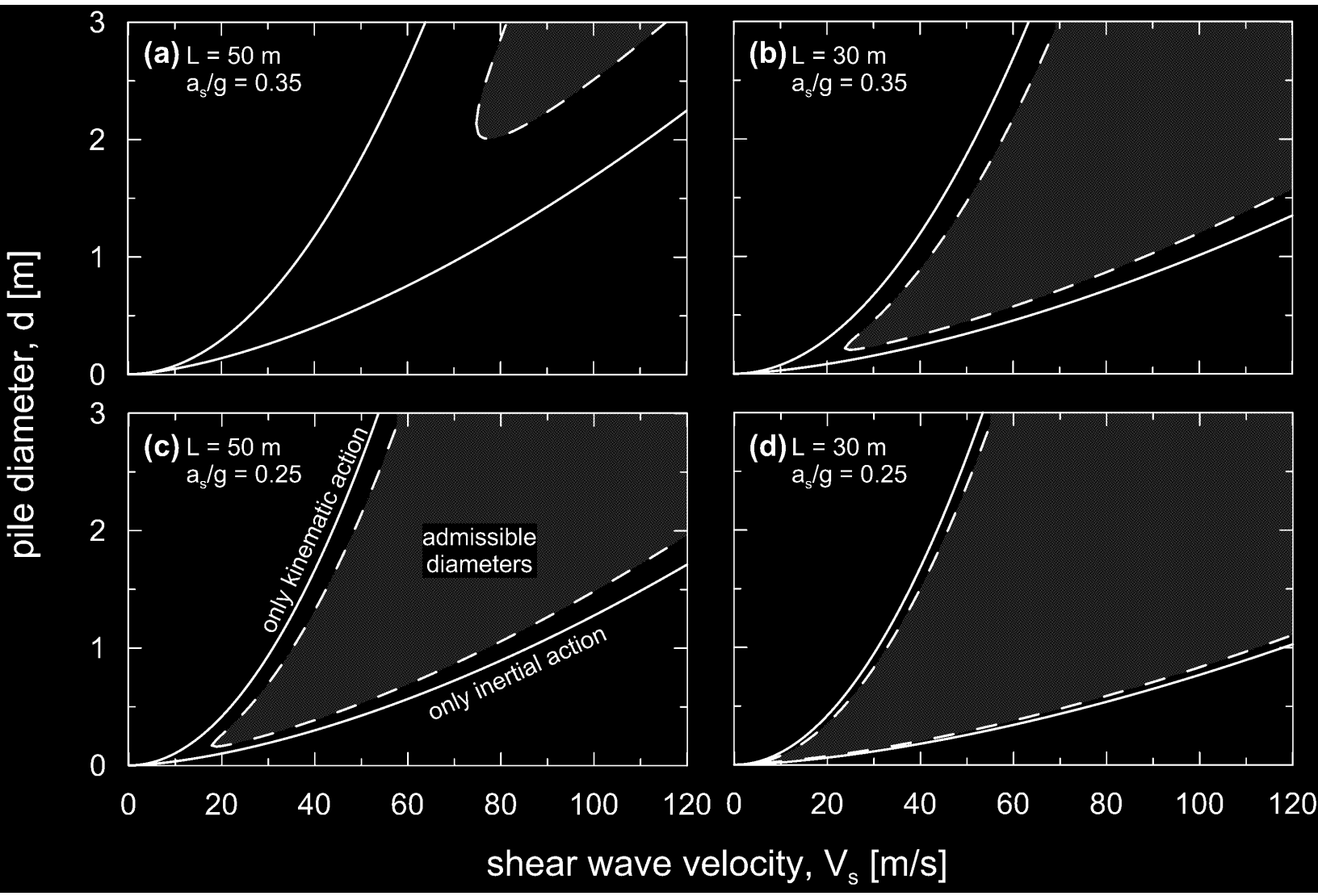
(a) L = 50 m
a_s/g = 0.35
(b) L = 30 m
a_s/g = 0.35
(c) L = 50 m
a_s/g = 0.25
(d) L = 30 m
a_s/g = 0.25
only kinematic action
admissible diameters
only inertial action
pile diameter, d [m]
shear wave velocity, V_s [m/s]
0
1
2
3
0
20
40
60
80
100
120

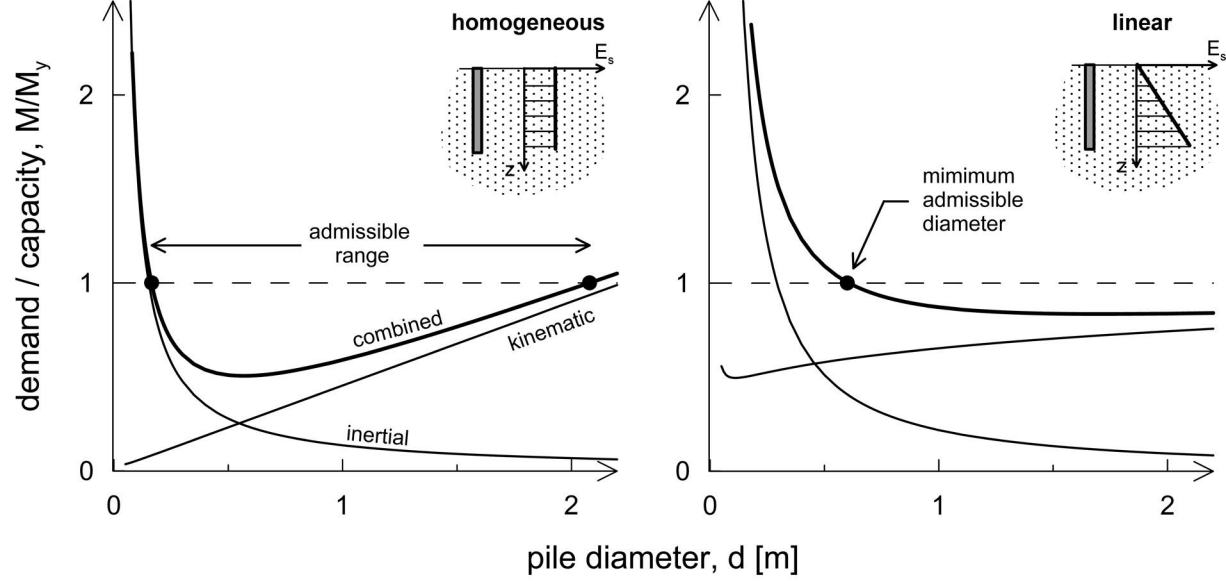
homogeneous
linear
E_s
z
admissible range
combined
kinematic
inertial
mimimum admissible diameter
demand / capacity, M/M_y
pile diameter, d [m]
0
1
2

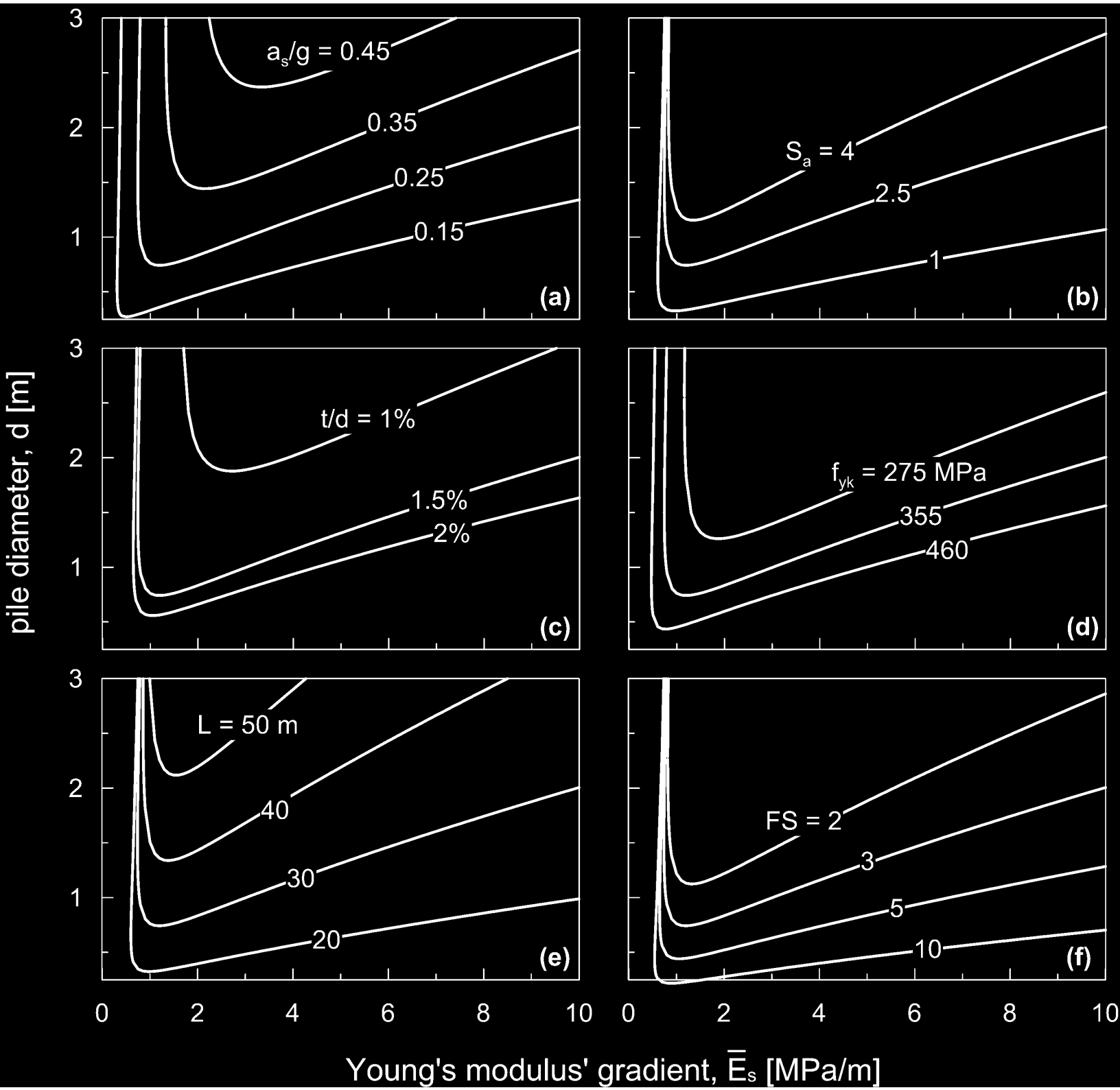
pile diameter, d [m]
Young's modulus' gradient, $\bar{E}_s$ [MPa/m]
a_s/g = 0.45
0.35
0.25
0.15
(a)
S_a = 4
2.5
1
(b)
t/d = 1%
1.5%
2%
(c)
f_{yk} = 275 MPa
355
460
(d)
L = 50 m
40
30
20
(e)
FS = 2
3
5
10
(f)
0
2
4
6
8
10
1
2
3

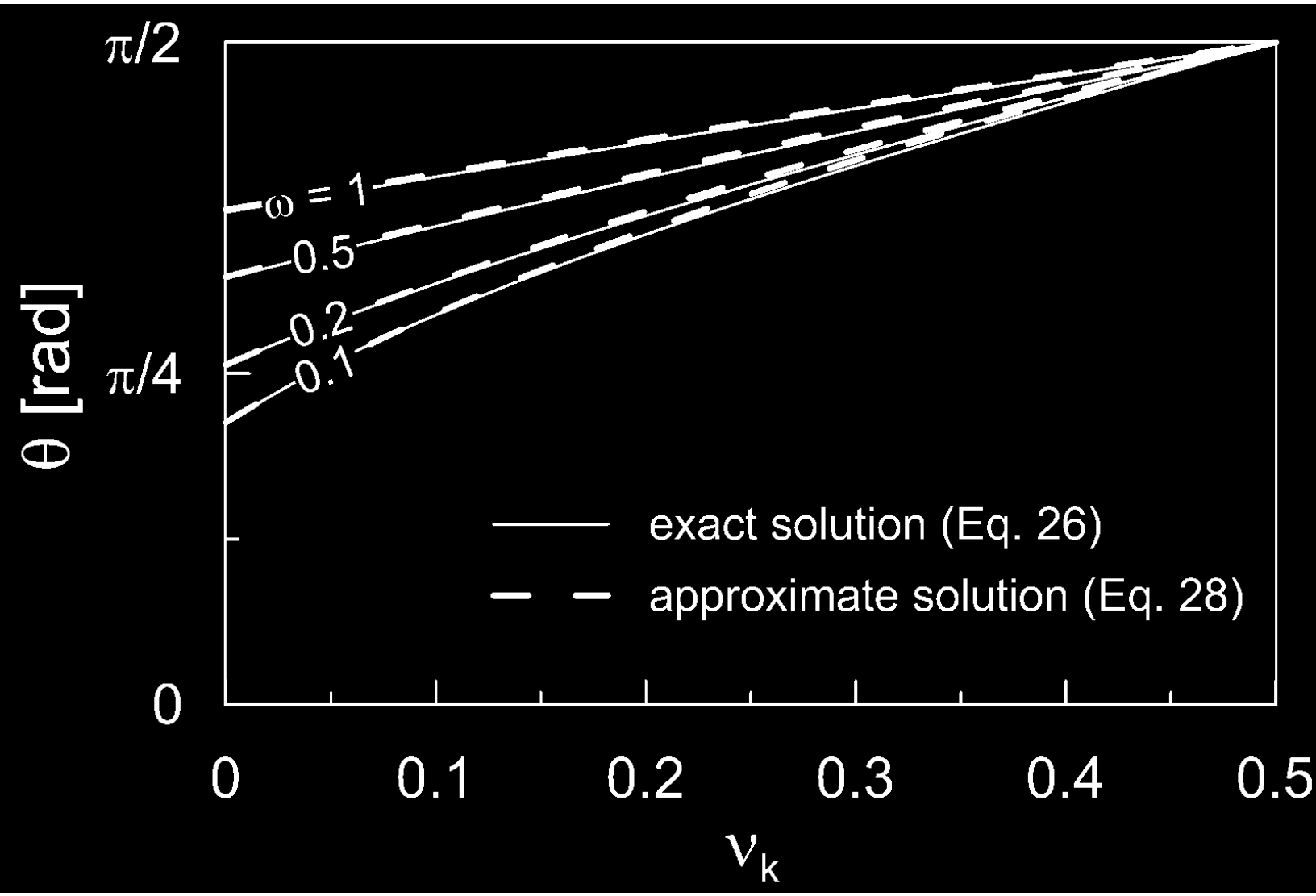
π/2
π/4
0
θ [rad]
ω = 1
0.5
0.2
0.1
exact solution (Eq. 26)
approximate solution (Eq. 28)
0
0.1
0.2
0.3
0.4
0.5
ν_k

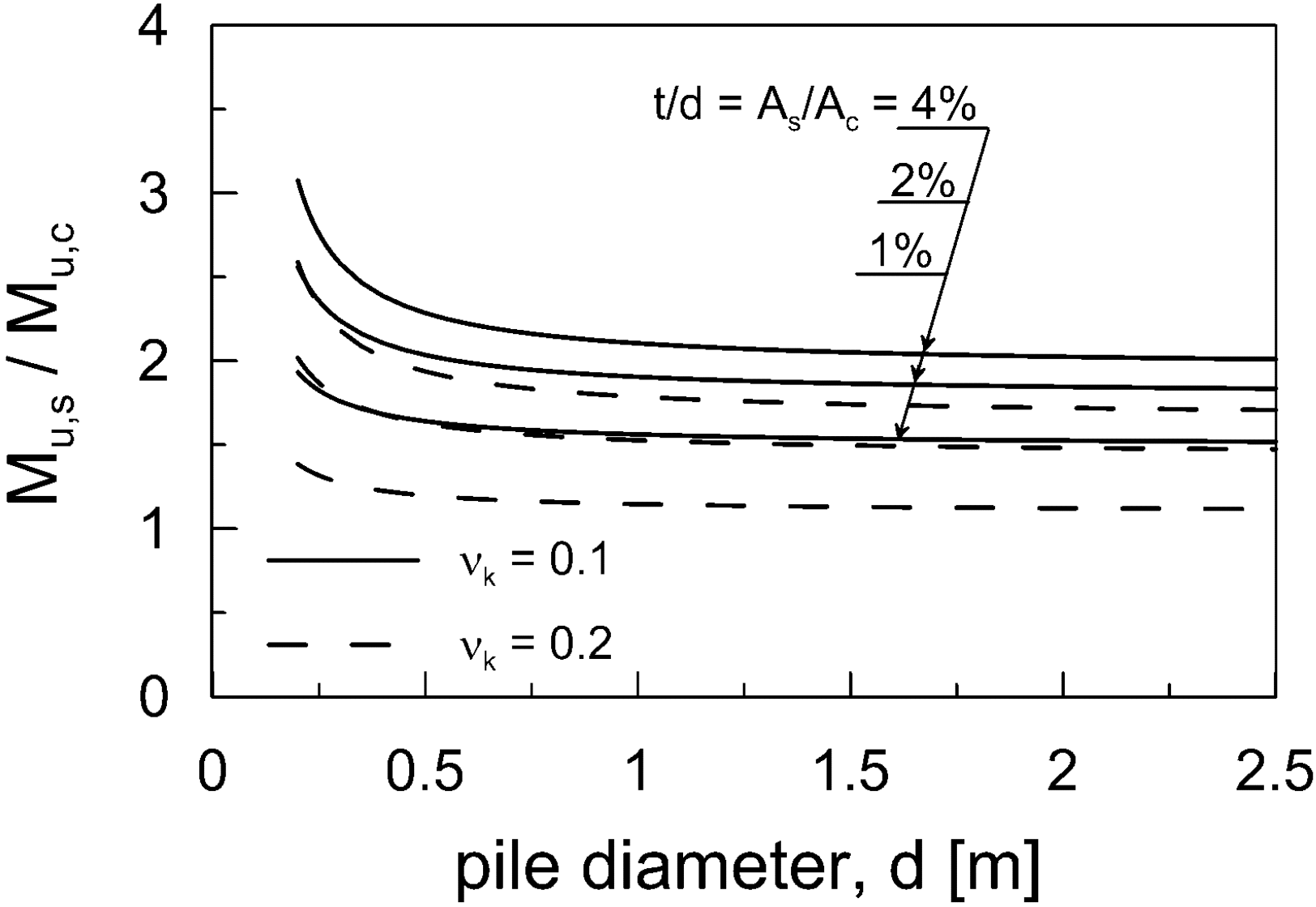
4
3
2
1
0
$M_{u,s}$ / $M_{u,c}$
t/d = A_s/A_c = 4%
2%
1%
ν_k = 0.1
ν_k = 0.2
0
0.5
1
1.5
2
2.5
pile diameter, d [m]

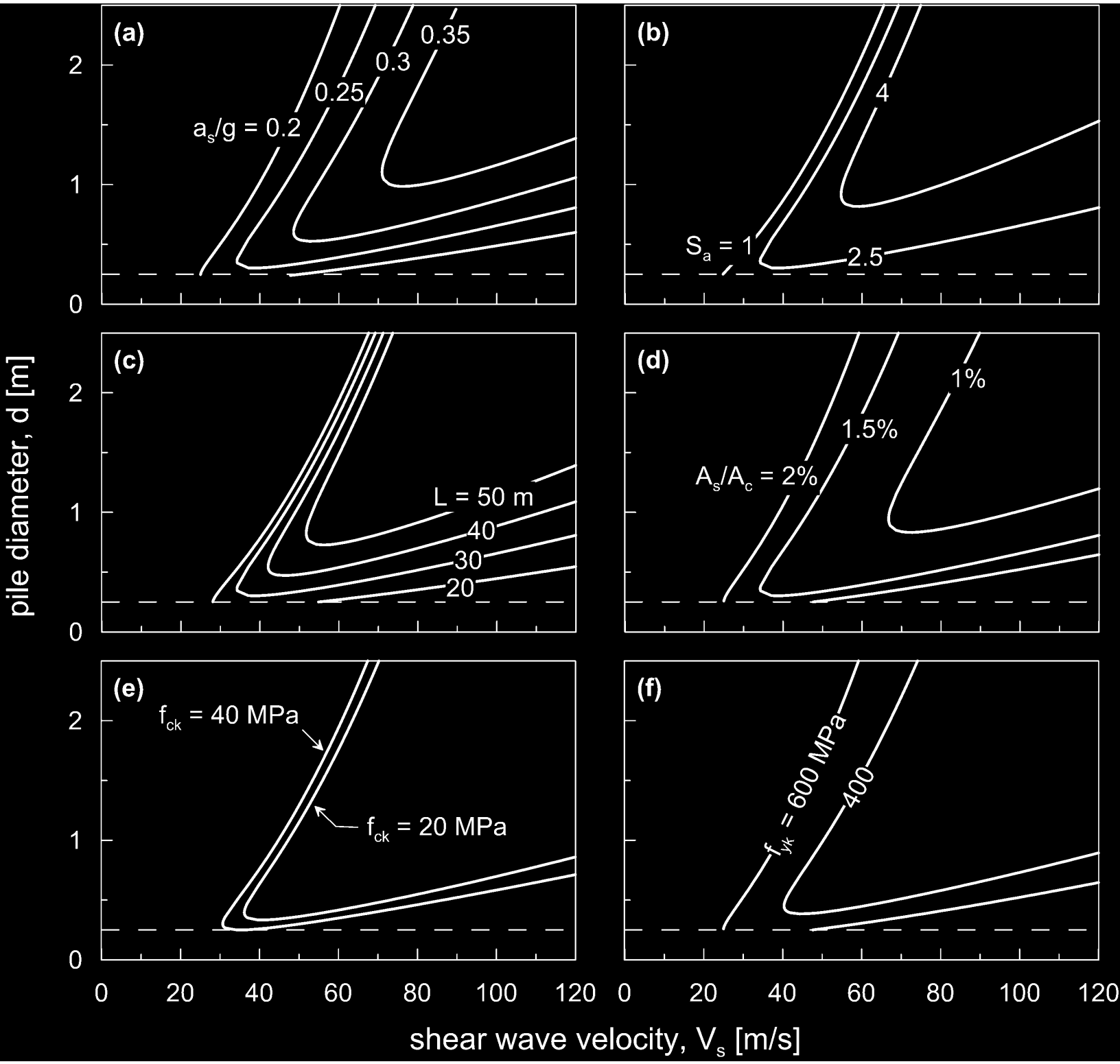
(a)
0.35
0.3
0.25
a_s/g = 0.2
(b)
4
S_a = 1
2.5
(c)
L = 50 m
40
30
20
(d)
1%
1.5%
A_s/A_c = 2%
(e)
f_{ck} = 40 MPa
f_{ck} = 20 MPa
(f)
f_{yk} = 600 MPa
400
pile diameter, d [m]
0
1
2
0
20
40
60
80
100
120
shear wave velocity, V_s [m/s]

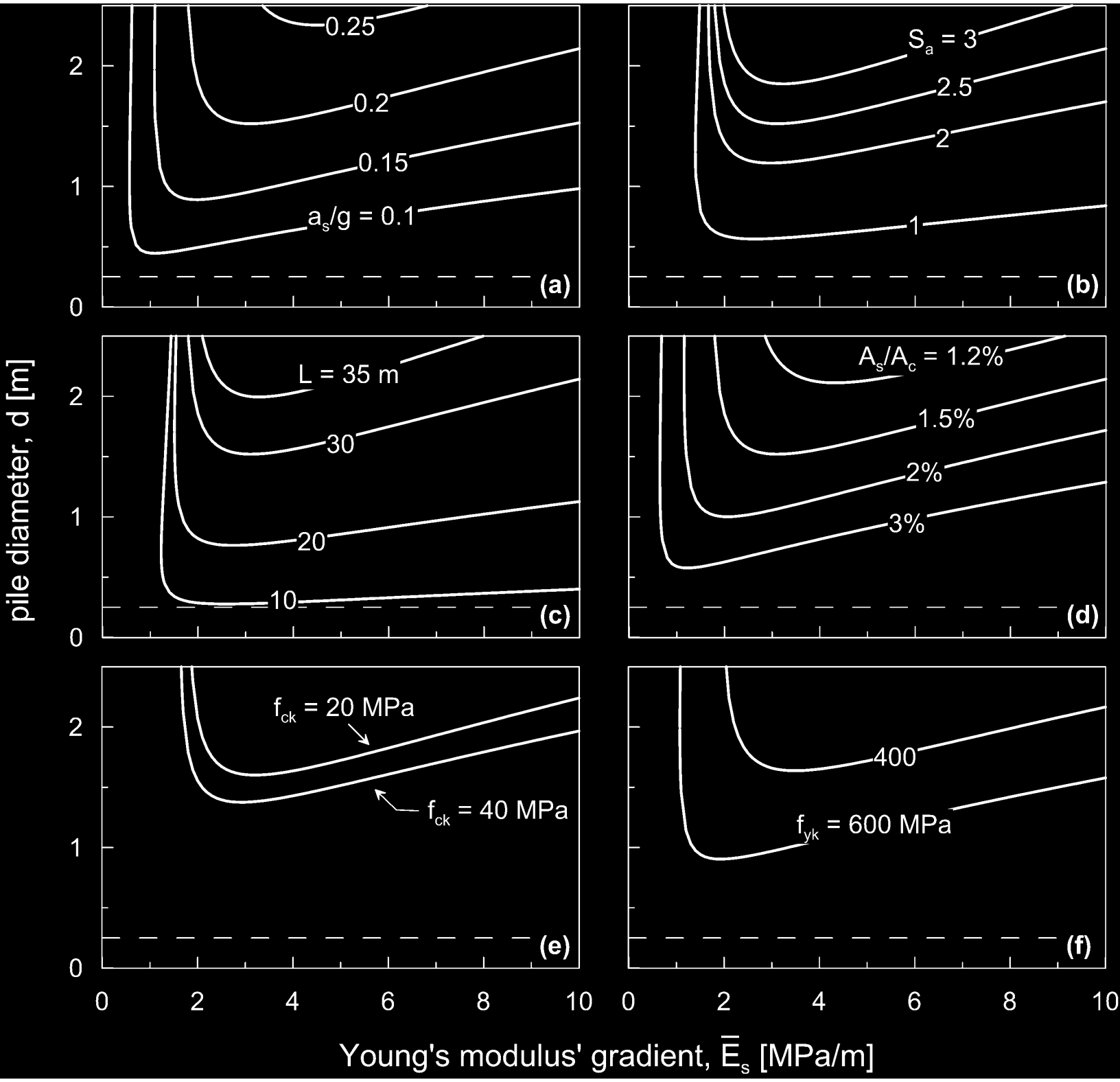
0.25
0.2
0.15
a_s/g = 0.1
(a)
S_a = 3
2.5
2
1
(b)
L = 35 m
30
20
10
(c)
A_s/A_c = 1.2%
1.5%
2%
3%
(d)
f_{ck} = 20 MPa
f_{ck} = 40 MPa
(e)
400
f_{yk} = 600 MPa
(f)
pile diameter, d [m]
0
1
2
0
2
4
6
8
10
Young's modulus' gradient, $\bar{E}_s$ [MPa/m]

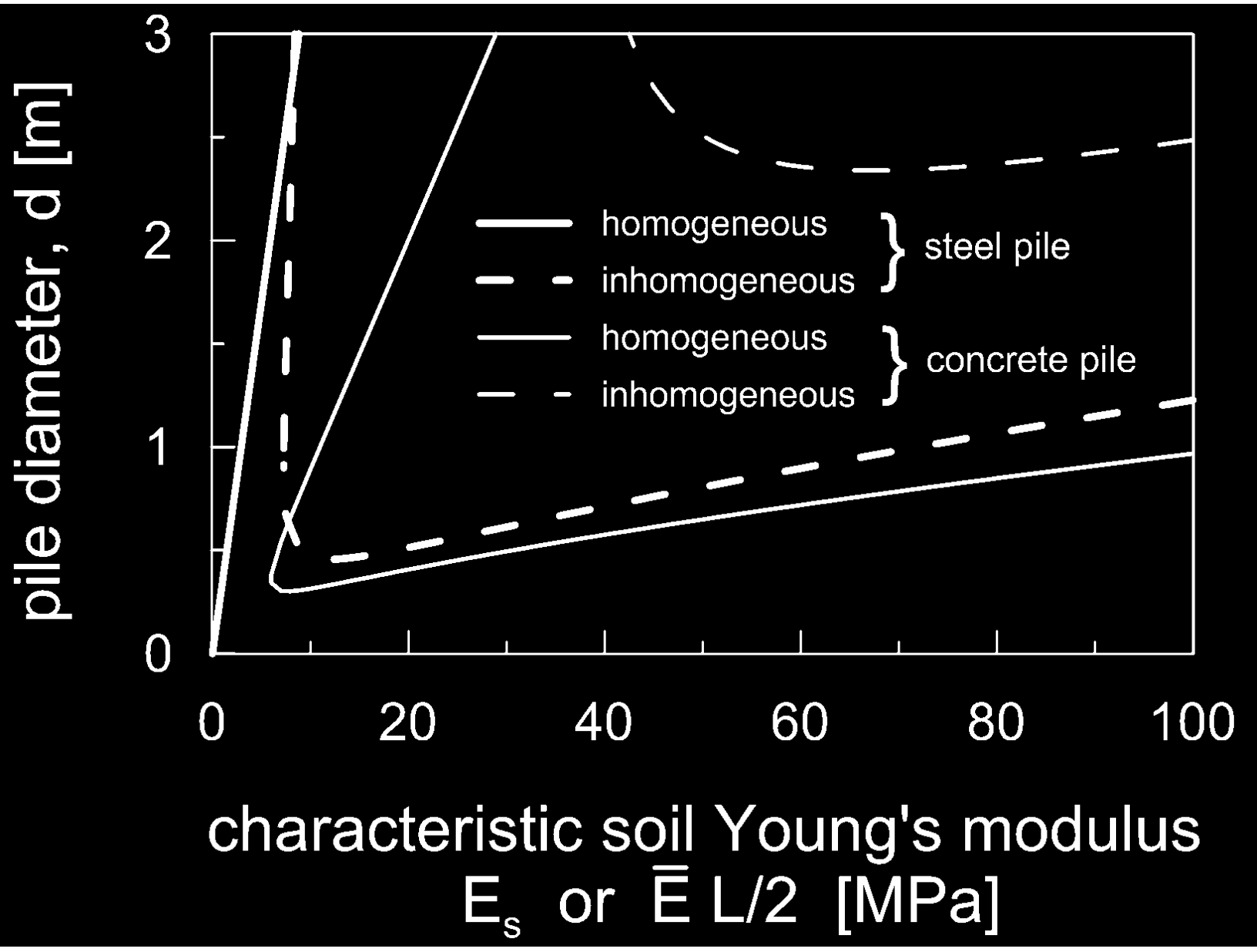
pile diameter, d [m]
3
2
1
0
0
20
40
60
80
100
homogeneous
inhomogeneous
steel pile
homogeneous
inhomogeneous
concrete pile
characteristic soil Young's modulus
E_s or $\bar{E}$ L/2 [MPa]